

SLAC-PUB-4937 Rev.
August 1991
(A)

Tolerances to Limit the Vertical Emittance in
Future Storage Rings*

T. O. RAUBENHEIMER

*Stanford Linear Accelerator Center
Stanford University, Stanford, California 94309*

Submitted to Particle Accelerator

* Work supported by Department of Energy contract DE-AC03-76SF00515.

Table of Contents

1.	INTRODUCTION	3
2.	PRELIMINARIES	6
2.1	Opening Angle	7
2.2	Equations of Motion	7
2.3	Perturbative Approximation	9
2.4	Errors	10
3.	CLOSED ORBIT	11
4.	VERTICAL DISPERSION	14
4.1	Vertical Dispersion	15
4.2	Random Errors	17
4.3	Orbit Errors	18
4.4	Beam Size	21
4.5	Simulations	22
5.	BETATRON COUPLING	25
5.1	Vertical Beam Size	26
5.2	Random Errors	30
5.3	Orbit Errors	32
5.4	Simulations	33
5.5	Non-Linear Coupling Effects	35
6.	CORRECTION	36
6.1	Vertical Dispersion	36
6.1.1	Global Correction – Emittance Correction	37
6.1.2	Local Correction	39
6.1.3	Measurement	40

6.2	Betatron Coupling	40
6.2.1	Global Correction – Emittance Correction	41
6.2.2	Local Correction	41
6.2.3	Measurement	43
6.3	Simulations	43
7.	DISTRIBUTIONS AND TOLERANCES	45
7.1	Emittance due to Vertical Dispersion	46
7.2	Emittance due to Betatron Coupling	49
7.3	Local Beam Size	52
7.4	Tolerances	53
8.	SUMMARY	54
9.	APPENDIX A	56
10.	APPENDIX B	61
11.	TABLES	68
12.	FIGURE CAPTIONS	70

ABSTRACT

Future synchrotron light sources and future damping rings for linear colliders will need to have very small vertical equilibrium emittances. In the limit of low beam current, the vertical emittance is primarily determined by the vertical dispersion and the betatron coupling. In this paper, the contributions to these effects from random misalignments and from a corrected closed orbit are calculated. In particular, contributions to the vertical emittance are carefully separated from contributions that only increase the vertical beam size; both of these effects are important in synchrotron light sources, but only the first contribution is important in a damping ring. Finally, the effectiveness of realistic correction techniques are calculated and their tolerances are derived to limit the vertical emittance with a 95% confidence level that are consistent these correction techniques.

1. INTRODUCTION

Future synchrotron light sources and damping rings for future linear colliders require very small vertical emittances and beam sizes. A small vertical emittance is required in future damping rings to maximize the luminosity of the linear collider while keeping the e^+/e^- beamstrahlung at a tolerable level. Small vertical beam sizes are needed in future synchrotron light sources to maximize the brightness and the spatial coherence of the photon beams.

In this paper, we discuss effects that contribute to both the vertical emittance and the vertical beam size in e^+/e^- storage rings; we differentiate between the two because it is possible to increase the beam size without increasing the emittance. Specifically, we consider contributions from the opening angle of the synchrotron radiation, the vertical dispersion, and the betatron coupling; we will neglect the effect of synchro-betatron resonances and all current dependent phenomena which also constrain the ring performance. The goal in performing this study is to illustrate how these effects contribute to the vertical emittance and beam size, and thereby determine the limitations that they impose on future designs. In particular, we will discuss alignment tolerances needed to limit the vertical emittance and beam size that are consistent with the inclusion of realistic correction techniques.

Ideally, the low current equilibrium emittance and beam size in an e^+/e^- storage ring is determined by two competing processes: quantum excitation and damping, both of which result from the synchrotron radiation emitted by the particles in the ring. The quantum excitation is due to the discrete nature of the radiation whereas the damping is a result of the mere existence of the synchrotron radiation.

The radiation of a photon changes the particle's energy and gives a small transverse kick that depends upon the opening angle of the radiation. The transverse kicks due to

the opening angle directly change the amplitude of the particles betatron motion, and thereby the bunch's emittance, while the change in energy due to the radiation has a more subtle effect. The particle executes betatron oscillations about a closed orbit in the ring. Since this closed orbit depends upon the particle energy, the radiation of a photon increases the rms amplitude of the betatron motion by displacing the closed orbit relative to the particle's position.¹ In the horizontal plane, the increase in emittance due this second effect is typically much larger than the increase due to the opening angle of the radiation, but ideally, in the vertical plane there is no dispersion and thus the opening angle should determine the vertical emittance.

In practice, this is not the case. First, vertical dipole errors and a non-zero vertical closed orbit in the quadrupole magnets will directly introduce vertical dispersion. Second, a non-zero vertical closed orbit through the sextupole magnets, vertical sextupole misalignments, or rotational misalignments of the quadrupoles couple the horizontal and vertical planes. This coupling has two effects both of which increase the vertical emittance. It couples the horizontal dispersion to the vertical, increasing the vertical, and it couples the x and y betatron motion so that energy is transferred between the two planes.

In this paper, the effects of the coupling on the vertical emittance and beam size are analyzed perturbatively, assuming a large aspect ratio ϵ_x/ϵ_y . In the next section, the relevant equations of motion are introduced. Then, in Section 3, we discuss the closed orbit and the closed orbit correlation function which will be needed to calculate the effects of a closed orbit.

In Section 4, we calculate the vertical emittance and beam size due to the vertical dispersion caused by random errors and a corrected closed orbit. In previous work, the corrected closed orbit has been treated either as a series of uncorrelated offsets in the

magnets^{2,3} or the same as an uncorrected closed orbit.^{4,5} Typically, the first procedure will overestimate the effect of the closed orbit and the second will underestimate the contribution.

Next, in Section 5, we use analogy with the vertical dispersion to discuss the betatron coupling. As stated, in an e^+/e^- ring the betatron coupling causes both a local beam size increase and a fundamental dilution of the vertical phase space. The coupling has been treated both exactly⁶⁻⁸ and when close to the linear coupling difference resonance.⁹⁻¹¹ Unfortunately, the first provides a formalism that is complex and does not lend itself to a simple understanding of the problem and the second approach is not sufficient when far from the coupling resonances, *i.e.*, weakly coupled. In particular, previous analysis of the betatron coupling suggests that the coupling can be corrected with a few (2-4) skew quadrupoles. This is not correct, one must correct the coupling at every bending magnet to fully correct the vertical emittance.

In Section 6, we estimate the effectiveness of various techniques in reducing the vertical emittance and beam size, comparing the analytic results with the results of simulations. Then, in Section 7, we discuss the calculation of tolerances, consistent with the correction techniques, to limit the vertical emittance and the beam size in future storage ring designs. The results of both Sections 6 and 7 are important when determining the tolerances to limit the vertical emittance with a specified degree of confidence.

Finally, it should be noted that many of the results in Sections 4 and 5, in particular, the effect of random errors, have been derived repeatedly over the last thirty years; references to the earlier sources are provided. The primary contributions in these sections are: the effects of a corrected closed orbit are calculated more precisely, the distinction between the local beam size increase and the emittance is emphasized, and a simple

form for the emittance due to betatron coupling is found which is analogous to the emittance due to the vertical dispersion. This later result is important for determining the effectiveness of the coupling correction which is discussed in Section 6. In addition, the distinction between the beam size and the emittance was obviously realized by the author of Ref. 3, but it seems to have been neglected in much of the literature. Since this is relevant in damping rings, it is important to emphasize the difference.

2. PRELIMINARIES

In this paper, we are interested in calculating both the vertical beam size and the vertical emittance; the beam size is the relevant quantity in some situations while the emittance is in others. We need to differentiate between the two because the vertical beam size is the *projection* of the beam's six-dimensional emittance onto the vertical plane. Thus, in addition to depending on the vertical emittance, the vertical beam size is also a function of the local coupling between the vertical plane and the horizontal and longitudinal planes. In the limit of weak coupling, this relation can be expressed as

$$\frac{\sigma_y^2(s)}{\beta_y(s)} = \epsilon_y + \frac{\sigma_{y\text{local}}^2(s)}{\beta_y(s)} \quad , \quad (2.1)$$

where $\sigma_{y\text{local}}$ includes the effects of the local coupling. Notice that the local coupling contribution to σ_y^2/β_y is a function of the azimuthal position in the ring s , while the contribution from the emittance is (approximately) invariant. This occurs because the emittance represents a fundamental dilution of the vertical phase space while σ_{local} is due to a coupling that can change from point-to-point.

At this point, we can further subdivide the contributions to the vertical beam size. As mentioned in the introduction, we consider three effects that contribute to the low current beam size: (1) the momentum dependence of the vertical closed orbit, *i.e.*, the

vertical dispersion, (2) the coupling of the betatron motion, and (3) the opening angle of the radiation. Since these three contributions are statistically independent, the vertical beam size can be written as the sum of the contributions,

$$\frac{\sigma_y^2(s)}{\beta_y(s)} = \frac{\sigma_{\beta \text{ coupling}}^2}{\beta_y} + \frac{\sigma_{\text{dispersion}}^2}{\beta_y} + \epsilon_{\text{opening ang.}} \quad (2.2)$$

Here, the first two contributions have both a local coupling contribution and an emittance contribution while the opening angle only contributes to the vertical emittance.

2.1 OPENING ANGLE

The last term in Eq. (2.2), the term due to the opening angle of the radiation, is small; a derivation is presented in Appendix A. It directly adds a contribution to the vertical emittance of

$$\epsilon_y = \frac{13}{55} C_q \frac{\oint \beta_y(s) |G^3(s)| ds}{\oint G^2(s) ds} \quad (2.3)$$

Here, $C_q = 3.84 \times 10^{-13} \text{m}$, β_y is the vertical beta function, and $G(s)$ is the inverse of the local bending radius. For comparison, in the damping rings currently being designed,¹² the desired vertical emittances are the order of 0.1 Å-rad and the opening angle contribution tends to be over an order of magnitude smaller. Obviously, as the desired ring emittances continue to decrease, the opening angle contribution will become significant, ultimately limiting the achievable low current emittance.

2.2 EQUATIONS OF MOTION

To calculate the other two contributions to the beam size, we will begin with equations for the vertical dispersion and the betatron motion. Neglecting the effects of syn-

chrotron radiation, the transverse equations of motion for a particle in a storage ring can be written¹³

$$\begin{aligned} x'' + (1 - \Delta) \left[(K_1 + G^2)x + \tilde{K}_1 y + \frac{K_2}{2}(x^2 - y^2) \right] &= \Delta G + (1 - \Delta)G_{xc} \\ y'' - (1 - \Delta) \left[K_1 y - \tilde{K}_1 x + K_2 xy \right] &= (1 - \Delta)G_{yc} \end{aligned} \quad (2.4)$$

Here, primes are used to denote derivatives with respect to s , the azimuthal coordinate. In addition, $\Delta = (p - p_0)/p$ where p_0 is the reference momentum, G is the main bending field, $G = 1/\rho(s)$ where ρ is the bending radius of an on-momentum particle, and G_{xc} and G_{yc} are the inverse bending radii of the dipole correctors. Finally, K_1 , \tilde{K}_1 , and K_2 are the normalized quadrupole, skew quadrupole, and sextupole fields, respectively:

$$K_1 = \frac{e}{p_0 c} \frac{\partial B_y}{\partial x}, \quad \tilde{K}_1 = \frac{e}{p_0 c} \frac{\partial B_x}{\partial x}, \quad K_2 = \frac{e}{p_0 c} \frac{\partial^2 B_y}{\partial x^2} \quad (2.5)$$

Note that with these definitions, K_1 is positive in horizontally focusing quadrupoles and positive $G_{xc}(G_{yc})$ increases $x'(y')$.

Now, the motion can be separated into three portions: a periodic closed orbit, it's first order energy dependance, *i.e.*, the dispersion function, and the betatron motion. Thus, $x = x_c + x_\beta + \delta\eta_x$, where δ is the energy deviation from the design energy. Using this expansion in Eq. (2.4), we find equations for the closed orbit

$$\begin{aligned} x_c'' + (K_1 + G^2)x_c + \tilde{K}_1 y_c + \frac{K_2}{2}(x_c^2 - y_c^2) &= G_{xc} \\ y_c'' - K_1 y_c + \tilde{K}_1 x_c - K_2 x_c y_c &= G_{yc} \end{aligned} \quad (2.6)$$

Next, linear equations for the dispersion function and the betatron motion can be found by expanding about the closed orbit:

$$\begin{aligned}
\eta_x'' + (K_1 + G^2)\eta_x + \tilde{K}_1\eta_y + K_2(x_c\eta_x - y_c\eta_y) = \\
G - G_{x_c} + (K_1 + G^2)x_c + \tilde{K}_1y_c + \frac{K_2}{2}(x_c^2 - y_c^2) \\
\eta_y'' - K_1\eta_y + \tilde{K}_1\eta_x - K_2(x_c\eta_y + y_c\eta_x) = \\
-G_{y_c} - K_1y_c + \tilde{K}_1x_c - K_2x_cy_c
\end{aligned} \tag{2.7}$$

and

$$\begin{aligned}
x_\beta'' + (K_1 + G^2)x_\beta + \tilde{K}_1y_\beta + K_2(x_cx_\beta - y_cy_\beta) = 0 \\
y_\beta'' - K_1y_\beta + \tilde{K}_1x_\beta - K_2(x_\beta y_c + x_c y_\beta) = 0 \quad ,
\end{aligned} \tag{2.8}$$

These equations are complicated. Although, we could solve for the coupled motion and beam sizes exactly,⁶⁻⁸ unfortunately, these exact solutions do not provide simple insight into the weakly coupled (flat beam) case. Thus, this paper will be limited to discussing flat beams and we will proceed by approximating these equations of motion.

2.3 PERTURBATIVE APPROXIMATION

In the limit of flat beams, one can solve the equations for the dispersion function and the betatron motion perturbatively. In this case, the horizontal dispersion must be much larger than the vertical $\eta_x \gg \eta_y$ and the horizontal emittance is much larger than the vertical $x_\beta \gg y_\beta$. Furthermore, without a loss in generality, we can assume that the horizontal closed orbit is zero; the effect of a non-zero horizontal closed orbit can be included by considering small changes of the focusing function K_1 due to the sextupoles.

Now, with these approximations, the equations for the dispersion and the betatron motion are

$$\begin{aligned}
x_\beta'' + (K_1 + G^2)x_\beta = 0 \\
y_\beta'' - K_1y_\beta = -\tilde{K}_1x_\beta + K_2y_cx_\beta \quad ,
\end{aligned} \tag{2.9}$$

and

$$\begin{aligned}\eta_x'' + (K_1 + G^2)\eta_x &= G \\ \eta_y'' - K_1\eta_y &= -G_{yc} - K_1y_c - \tilde{K}_1\eta_x + K_2y_c\eta_x\end{aligned}\tag{2.10}$$

These equations are no longer coupled, the vertical motion is simply driven by the horizontal, and thus they are simple to solve.

2.4 ERRORS

As has been mentioned, excluding the opening angle contribution, the low current vertical beam size is determined by errors in an uncoupled storage ring. In this paper, we will consider the effect of random vertical misalignments of the quadrupoles, sextupoles, and the Beam Position Monitors (BPMs). In addition, we will also consider the effect of random rotational errors of the quadrupoles and the bending dipoles. The effect of these errors is summarized in Table 1 where y_m and Θ are the vertical and rotational misalignments. As one can see from Eqs. (2.9) and (2.10), vertical dipole errors, due to rotations of the bends, vertical misalignments of the quadrupoles, or a non-zero closed orbit in the quadrupoles, directly introduces vertical dispersion. In addition, these same dipole errors create a non-zero vertical closed orbit which couples the x and y planes in the sextupoles. Finally, quadrupole rotations and sextupole misalignments will also couple the two transverse planes. We will discuss these effects in detail in Sections 4 and 5 after discussing the closed orbit in the next section.

3. CLOSED ORBIT

In this section, we calculate the closed orbit and the closed orbit correlation function resulting from the misalignments. The correlation function will be needed to calculate the beam sizes resulting from the vertical dispersion and the betatron coupling. Although this paper is primarily concerned with the effects of corrected orbits, we will derive expressions for both corrected and uncorrected orbits for comparison.

The vertical close orbit is described by Eq. (2.6). Assuming that the skew quadrupole terms are small, *i.e.*, the weak coupling limit, Eq. (2.6) is easily solved with the periodic Greens function for the ring:

$$\mathcal{G}_{x,y}(s, s') = \frac{\sqrt{\beta_{x,y}(s)\beta_{x,y}(s')}}{2 \sin \pi \nu_{x,y}} \cos(|\psi_{x,y}(s) - \psi_{x,y}(s')| - \pi \nu_{x,y}) \quad , \quad (3.1)$$

where, β is the beta function, ν is the tune, and ψ is the phase advance: $\psi = \int ds/\beta$. Using this, we find a solution for the vertical closed orbit,

$$y_c(s) = \frac{\sqrt{\beta_y(s)}}{2 \sin \pi \nu_y} \int_s^{s+C} \sqrt{\beta_y(z)} \cos(\psi_y(s) - \psi_y(z) + \pi \nu_y) G(z) dz \quad (3.2)$$

where $G(s) = G_{yc} + G\Theta_B + K_1 y_m$.

Now, we can calculate the expected rms magnitude of the closed orbit given an ensemble of random dipole errors, with a Gaussian distributions. One finds the well known result¹⁴

$$\langle y_c^2(s) \rangle = \frac{\beta_y(s)}{8 \sin^2 \pi \nu_y} \sum_{kicks} \langle G^2 L^2 \rangle \overline{\beta_y} \quad , \quad (3.3)$$

where the beta function at each kick is approximated by the average beta function within that magnet and the angle brackets are used to denote the expected value which is found by averaging over the gaussian distribution of errors.

Next, to calculate the vertical dispersion and the coupling introduced by the errors, we need the correlation function for the closed orbit, $\langle y_c(s')y_c(s) \rangle$. Using Eq. (3.2), this can be expressed as a double integral

$$\langle y_c(s')y_c(s) \rangle = \frac{\sqrt{\beta(s)\beta(s')}}{4 \sin^2 \pi \nu} \int_{s'}^{s'+C} dz' \int_s^{s+C} dz \sqrt{\beta' \beta} \langle G(z')G(z) \cos' \cos \rangle \quad , \quad (3.4)$$

where $\beta' = \beta(z')$, $\cos = \cos(\psi(s) - \psi(z) + \pi \nu)$, and $\cos' = \cos(\psi(s') - \psi(z') + \pi \nu)$. To evaluate $\langle G(z')G(z) \rangle$ the integrals must be over the same portion of the ring. Assume initially that $s' > s$, then

$$\langle y_c(s')y_c(s) \rangle = \frac{\sqrt{\beta(s)\beta(s')}}{4 \sin^2 \pi \nu} \left[\int_{s'}^{s+C} \int_{s'}^{s+C} dz' dz \dots + \int_{s+C}^{s'+C} dz' \int_s^{s'} dz \dots \right] \quad , \quad (3.5)$$

where \dots is used to represent the integrands. As before the double integrals collapse to single sums over the kicks, but the second double integral has different limits and thus an additional factor of $2\pi\nu$ must be added to the phase $\psi(z')$. We average over the high frequency terms and, in the case of an uncorrected closed orbit, we are left with

$$\begin{aligned} \langle y_c(s')y_c(s) \rangle = & \frac{\sqrt{\beta_y(s)\beta_y(s')}}{8 \sin^2 \pi \nu_y} \left[\cos \Delta\psi \sum_{i=s}^{s+C} \beta_{yi} \langle G_i^2 L_i^2 \rangle \right. \\ & \left. + \left(\cos(|\Delta\psi| - 2\pi\nu_y) - \cos \Delta\psi \right) \left| \sum_{i=s}^{s'} \beta_{yi} \langle G_i^2 L_i^2 \rangle \right| \right] \quad , \quad (3.6) \end{aligned}$$

where $\Delta\psi = \psi_y(s') - \psi_y(s)$ and the absolute values signs were used to include the case $s' < s$. Note that terms of order $1/4\pi\nu_y$ have been dropped from Eq. (3.6); these will be small corrections in high tune, low emittance rings.

We consider two cases: an uncorrected orbit and the orbit after substantial correction. Since the correlation function is periodic in Δs , we can express it as a fourier

series. Furthermore, it must be an even function of Δs and thus the fourier series will only contain cosine terms:

$$\langle y_c(s')y_c(s) \rangle = \sqrt{\beta_y(s)\beta_y(s')} \frac{\langle y^2 \rangle}{\beta_y} \left[\frac{c_0}{2} + \sum_{n=1}^{\infty} c_n \cos \frac{n\Delta\psi}{\nu_y} \right] \quad (3.7)$$

To calculate the coefficients c_n for an uncorrected orbit, we make a smooth approximation

$$\left| \sum_{i=s}^{s'} \beta_{yi} \langle G_i^2 L_i^2 \rangle \right| \approx \frac{|\Delta\psi|}{2\pi\nu_y} \sum_{i=s}^{s+C} \beta_{yi} \langle G_i^2 L_i^2 \rangle \quad , \quad (3.8)$$

where $\Delta\psi = \psi(s') - \psi(s)$. The coefficients are then

$$c_n = \frac{(n^2 + \nu_y^2)(1 - \cos 2\pi\nu_y)}{\pi^2(n^2 - \nu_y^2)^2} \quad (3.9)$$

Here, only the two harmonics c_n on either side of the tune, $n = \lfloor \nu_y \rfloor, \lceil \nu_y \rceil$, will be large, and thus, we can approximate the uncorrected orbit with just these two terms.

When the closed orbit is corrected its Fourier spectrum tends towards that of white noise. There are two reasons for this: first, most orbit correction techniques tend to reduce the dominant harmonics on either side of the tune while increasing the other modes. The second, and more fundamental, reason is that the Beam Position Monitors (BPMs) are misaligned relative to the ring centerline. Thus, even with perfect orbit correction, where the measured orbit is zeroed at all of the position monitors, the *actual* closed orbit will have a white noise spectrum.

We can approximate this by assuming that the correctors “randomize” the orbit and thus points on either side of a corrector are uncorrelated. Furthermore, in the limit of a

very corrected orbit, *i.e.* one with many correctors, we can approximate the correlation function between correctors with just the first term of Eq. (3.6). Thus,

$$\langle y_c(s')y_c(s) \rangle_{\text{cor}} = \sqrt{\beta_y(s)\beta_y(s')} \frac{\langle y_c^2 \rangle}{\beta_y} \begin{cases} \cos \Delta\psi, & \text{No correctors} \\ & \text{between } s \text{ and } s' \\ 0, & \text{Otherwise} \end{cases} \quad (3.10)$$

Here, the term $\langle y_c^2 \rangle / \beta_y$ is not equal to Eq. (3.3), it is the square of the *residual* orbit after correction. In particular, for an orbit that is fully corrected, one can approximate $\langle y_c^2 \rangle$ with the estimated vertical misalignments of the BPMs $\langle y_m^2 \rangle$.

4. VERTICAL DISPERSION

The vertical dispersion increases the beam size in two ways: first, the vertical dispersion results from a coupling between the longitudinal energy deviation and the vertical position. Since the beam contains a finite energy spread, the vertical dispersion directly contributes to the vertical beam size. This will be referred to as the “local” contribution since the beam size increase only depends upon the local value of the vertical dispersion; the energy spread in the beam does not vary significantly around the ring.

The second effect of the vertical dispersion is more subtle. Particles traverse the ring performing betatron oscillations about a closed orbit which is energy dependant; this energy dependance is the vertical dispersion. When a synchrotron photon is emitted, the particle’s longitudinal energy changes, causing it’s closed orbit to change. This changes the amplitude and phase of the betatron oscillation; the particle oscillates about the new closed orbit. Since the photons are uncorrelated, the radiation causes an increase in the rms amplitude of the betatron oscillation.¹ This effect will be referred to as the “global” contribution of the vertical dispersion since the effect depends upon the value of the dispersion in all of the bending magnets.

Although, both the local and the global contributions from the vertical dispersion increase the vertical beam size, there is a fundamental difference between the two. The local effect is simply due to a coupling between the longitudinal and vertical planes; it does not actually change the beam's six-dimensional emittance. In contrast, the global effect of the dispersion does cause an increase in the beam emittance. In a synchrotron light source, the distinction between the local and global effects is irrelevant; one is only interested in projected beam size. But, in a damping ring, the distinction is important since there one is interested in the extracted beam *emittance*; in theory, any residual coupling can be removed.

To calculate these two effects, we will first derive expressions for the dispersion arising from random errors and a non-zero closed orbit. Then, we will calculate the contributions to the vertical beam size and the emittance. Finally, the calculations will be compared with the results of simulations.

4.1 VERTICAL DISPERSION

To find the vertical beam size contribution due to dispersion, we need to first solve for the vertical dispersion and its derivative. In the limit of flat beams, the vertical dispersion is given by:

$$\begin{aligned}\eta_x'' + (K_1 + G^2)\eta_x &= G \\ \eta_y'' - K_1\eta_y &= -G_{yc} - K_1y_c - \tilde{K}_1\eta_x + K_2y_c\eta_x\end{aligned}\tag{2.10}$$

These equations are solved in the same manner as the equation for the closed orbit, namely, by using the periodic Greens function for the focusing field of the ring, Eq. (3.1).

The solutions are¹⁴

$$\begin{aligned}\eta_x(s) &= \frac{\sqrt{\beta_x(s)}}{2 \sin \pi \nu_x} \int_s^{s+C} \sqrt{\beta_x(z)} \cos(\psi_x(s) - \psi_x(z) + \pi \nu_x) G(z) dz \\ \eta_y(s) &= \frac{\sqrt{\beta_y(s)}}{2 \sin \pi \nu_y} \int_s^{s+C} \sqrt{\beta_y(z)} \cos(\psi_y(s) - \psi_y(z) + \pi \nu_y) F(z) dz\end{aligned}\tag{4.1}$$

where $G(s)$ is the main bending function and $F(s) = (K_2 \eta_x - K_1) y_c - \tilde{K}_1 \eta_x - G_{yc}$.

Now, the derivative of η_y with respect to s can be found directly from Eq. (4.1). Unfortunately, this is complicated by the beta function which is also a function of s . Instead, the function η_y^* , which is a function of η_y and its derivative, is introduced:³

$$\eta_y^*(s) \equiv \alpha_y \eta_y + \beta_y \eta_y' \tag{4.2}$$

This function is convenient since it both simplifies the expression for the vertical emittance and has a solution that can be expressed in a form similar to (4.1):

$$\eta_y^*(s) = -\frac{\sqrt{\beta_y(s)}}{2 \sin \pi \nu_y} \int_s^{s+C} \sqrt{\beta_y(z)} \sin(\psi_y(s) - \psi_y(z) + \pi \nu_y) F(z) dz \tag{4.3}$$

Because the two equations have similar forms, the calculation of η_y^{*2} will parallel that of η_y^2 . In particular, we will see that for random errors the expected values of η_y^2 and η_y^{*2} are equal.

4.2 RANDOM ERRORS

To estimate the beam size contribution, we need to calculate the expected values of η_y^2/β_y and η_y^{*2}/β_y for the various error distributions. The square of the vertical dispersion, Eq. (4.1), is a double integral

$$\frac{\langle \eta_y^2 \rangle}{\beta_y} = \frac{1}{4 \sin^2 \pi \nu_y} \int_s^{s+C} \int dz dz' \sqrt{\beta \beta'} \langle \cos \cos' F^2(z, z') \rangle \quad (4.4)$$

where β' , \cos , and \cos' are defined as they were in Eq. (3.4). In addition, since the errors considered, quadrupole rotations, sextupole misalignments, and dipole errors, are all assumed to be statistically independent, the function $F^2(z, z')$ contains five terms

$$\begin{aligned} \langle F^2(z, z') \rangle = & 4K_1 \eta_x K_1' \eta_x' \langle \Theta \Theta' \rangle + K_2 \eta_x K_2' \eta_x' \langle y_m y_m' \rangle \\ & + \langle G_y G_y' \rangle - 2f' \langle G_y y_c' \rangle + f f' \langle y_c y_c' \rangle \quad , \end{aligned} \quad (4.5)$$

where the primes are used to denote functions of z' instead of z . In addition, $f(z)$ is proportional to the *local* chromaticity, $f(z) = K_2 \eta_x - K_1$. The chromaticity is given by¹⁴

$$\xi_y \equiv \frac{d\nu_y}{dp/p_0} = \frac{1}{4\pi} \oint (K_1 - K_2 \eta_x) \beta_y ds \quad . \quad (4.6)$$

It is important to notice that the vertical dispersion due to a closed orbit can be reduced by using *local* chromatic correction which reduces $f(z)$; this will be discussed further in the next section.

Since the errors are uncorrelated, the first three terms of Eq. (4.4) are calculated in the same manner as $\langle y_c^2 \rangle / \beta_y$, Eq. (3.3), yielding the results¹⁴

$$\begin{aligned} \frac{\langle \eta_y^2 \rangle_{\text{quad rotation}}}{\beta_y} &= \frac{1}{8 \sin^2 \pi \nu_y} \sum_{\text{quad}} (K_1 L)^2 4 \Theta^2 \beta_y \eta_x^2 \\ \frac{\langle \eta_y^2 \rangle_{\text{sext misalign}}}{\beta_y} &= \frac{1}{8 \sin^2 \pi \nu_y} \sum_{\text{sext}} (K_2 L)^2 y_m^2 \beta_y \eta_x^2 \quad , \end{aligned} \quad (4.7)$$

$$\frac{\langle \eta_y^2 \rangle_{\text{dipole kicks}}}{\beta_y} = \frac{\langle y_c^2 \rangle}{\beta_y} \quad (4.8)$$

All of the above equations are applicable for both corrected or uncorrected orbits. The first two do not depend upon the closed orbit and the term $\langle y_c^2 \rangle / \beta_y$ in the third equation is equal to Eq. (3.3) for an uncorrected orbit or the square of the *residual* for a corrected orbit. Notice that this third term is not a result of a non-zero closed orbit; it results from the errors that create the non-zero closed orbit.

Finally, note that we have calculated the expected value of $\langle \eta_y^2 \rangle / \beta_y$, but to calculate the emittance we will also need to calculate $\langle \eta_y^{*2} \rangle / \beta_y$. As mentioned, this is quantity calculated in an analogous manner; it differs from $\langle \eta_y^2 \rangle / \beta_y$ in that \cos and \cos' become \sin and \sin' , but with the same approximations, the results are identical.

4.3 ORBIT ERRORS

The fourth and fifth terms of Eq. (4.4) are functions of the closed orbit. We will treat each of these terms in turn. First, we express the fourth term as an integral of the closed orbit correlation function:

$$\left(\frac{\langle \eta_y^2 \rangle}{\beta_y} \right)_4 = \frac{-2}{2\sqrt{\beta(s)} \sin \pi \nu} \int_s^{s+C} f' \sqrt{\beta'_y(z')} \cos' \langle y_c(s) y_c(z') \rangle dz' \quad , \quad (4.9)$$

where the subscript 4 is used to denote that this is the fourth term of Eq. (4.5).

Next, using the fourier expansion for the closed orbit function, Eq. (3.7), we calculate this integral. In addition, since we are not interested in the explicit dependence on position, we can average over s . This yields

$$\overline{\left(\frac{\langle \eta_y^2 \rangle}{\beta_y} \right)_4} = 2\xi_y \frac{\langle y_c^2 \rangle}{\beta_y} \sum_{n,\pm} \frac{c_n}{\nu_y \pm n} \quad , \quad (4.10)$$

where ξ_y is the chromaticity defined in Eq. (4.6) and the \pm is used to represent a sum over both $1/(\nu_y+n)$ and $1/(\nu_y-n)$. Now, if we only keep the most significant coefficients c_n for an uncorrected orbit, this becomes

$$\overline{\left(\frac{\langle \eta_y^2 \rangle}{\beta_y}\right)}_4 \approx \frac{2\pi\xi_y}{\sin \pi\nu_y} \frac{\langle y_c^2 \rangle}{\beta_y} \text{sinc}^3 \pi\Delta\nu_y \quad (4.11)$$

where $\Delta\nu_y$ is the fractional part of the tune and $\text{sinc } x = \sin x/x$.

We can calculate this term for a corrected orbit in a similar manner. This yields

$$\overline{\left(\frac{\langle \eta_y^2 \rangle}{\beta_y}\right)}_4 \approx \frac{2\pi\xi_y}{\sin \pi\nu_y} \frac{\langle y_c^2 \rangle}{\beta_y} \frac{\cos \pi\nu_y}{N_{\text{cor}}} \quad (4.12)$$

Here, N_{cor} is equal to the number of correctors which we have assumed are uniformly distributed. Notice that, although the corrected result is smaller by $1/N_{\text{cor}}$, the forms of the corrected and uncorrected results are similar. In particular, note that both results depend linearly upon the chromaticity ξ_y which is usually adjusted to be small and thus both Eqs. (4.11) and (4.12) will tend to be small.

Now, we turn to the last term in Eq. (4.4). This contains the closed orbit correlation function, Eq. (3.6). To solve for the effect of an uncorrected orbit, we again use the fourier expansion for the correlation function. This yields

$$\left(\frac{\langle \eta_y^2 \rangle}{\beta_y}\right)_5 = \frac{1}{4 \sin^2 \pi\nu_y} \frac{\langle y_c^2 \rangle}{\beta_y} \int_s^{s+C} \int dz dz' f f' \beta_y \beta_y' \cos \cos' \sum_n c_n \cos \frac{n\Delta\psi}{\nu_y} \quad , \quad (4.13)$$

where $\Delta\psi = \psi(z) - \psi(z')$. This expression is evaluated in the same manner as the previous case; we first calculate the integrals and then average over s . We find

$$\begin{aligned} \overline{\left(\frac{\langle \eta_y^2 \rangle}{\beta_y}\right)}_5 &= \frac{1}{16 \sin^2 \pi\nu_y} \frac{\langle y_c^2 \rangle}{\beta_y} \sum_{n=0}^{\infty} c_n \left[\left| \int_0^C dz f \beta_y e^{i\psi(1-n/\nu_y)} \right|^2 \right. \\ &\quad \left. + \left| \int_0^C dz f \beta_y e^{i\psi(1+n/\nu_y)} \right|^2 \right] \quad . \end{aligned} \quad (4.14)$$

We can approximate this by assuming that the fractional tune $\Delta\nu_y$ is small and thus we keep only the most significant coefficient c_n . This yields

$$\overline{\left(\frac{\langle\eta_y^2\rangle}{\beta_y}\right)}_5 \approx \frac{1}{16 \sin^2 \pi \nu_y} \frac{\langle y_c^2 \rangle}{\beta_y} \text{sinc}^4 \pi \Delta \nu_y \left((4\pi \xi_y)^2 + (4\pi \Delta)^2 \right) , \quad (4.15)$$

where Δ is

$$\Delta = \frac{1}{4\pi} \left| \int_0^C dz f \beta_y e^{i2\psi} \right| , \quad (4.16)$$

and is sometimes referred to as the width of the off-energy stop band. This result is similar to the result found in Ref. 5. The primary difference is in the appearance of the coefficients although they actually have the same value over much of the range.

Finally, we solve for the effect of a corrected orbit in a similar manner, finding

$$\overline{\left(\frac{\langle\eta_y^2\rangle}{\beta_y}\right)}_5 \approx \frac{1}{16 \sin^2 \pi \nu_y} \frac{\langle y_c^2 \rangle}{\beta_y} \sum_{n_c}^{N_{cor}} \left[\left| \int_{n_c}^{n_c+1} dz f \beta_y \right|^2 + \left| \int_{n_c}^{n_c+1} dz f \beta_y e^{i2\psi} \right|^2 \right] , \quad (4.17)$$

where n_c denotes the position of one corrector and n_c+1 denotes the position of the next corrector. This result differs significantly from the uncorrected case. The uncorrected case depends on the average values of $f\beta_y$ and $f\beta_y e^{i2\psi}$. In general, these will be small; the former, the chromaticity, is usually small by design while the later tends to be small because of the oscillating term $e^{i2\psi}$. In contrast, the corrected case depends on what is referred to as the *local* chromaticity and the *local* Δ . Both of these will typically be much larger than the average values. The local chromaticity is usually positive in regions of dispersion to compensate the negative values in the dispersion free regions. While the average may be zero, the local values are not. In addition, the local value of Δ will tend to be much larger than the average since the oscillating term does not vary significantly over a short region.

Of course, despite the larger values of ξ_{local} and Δ_{local} , the dispersion of the corrected orbit will usually be smaller than that of an uncorrected orbit; orbit correction reduces the residual orbit $\langle y_c^2 \rangle / \beta$. Furthermore, if the closed orbit is comparable in magnitude to the misalignments $y_c \approx y_m$, the contribution to the vertical dispersion from the closed orbit will usually be much *less* than that from the misalignments. This occurs because the orbit, even after correction, is still correlated for short segments and some of the quadrupole and sextupole deflections cancel.

4.4 BEAM SIZE

At this point, we can solve for the beam size increase due to the vertical dispersion. As mentioned, the vertical dispersion has two effects: (1) it directly increases the beam size by coupling a particle's energy deviation to its vertical position, and (2) it causes the vertical emittance to increase. The first effect is simple; it causes a local contribution to the expected beam size of

$$\frac{\langle \sigma_y^2(s) \rangle_{\text{local}}}{\beta_y(s)} = \frac{\langle \eta_y^2(s) \rangle}{\beta_y(s)} \sigma_\epsilon^2 \quad (4.18)$$

where σ_ϵ is the rms energy deviation in the beam.

To calculate the second effect, the emittance increase, we use the Courant-Snyder invariant \mathcal{H}_y which can be expressed

$$\mathcal{H}_y(s) = \frac{1}{\beta_y} (\eta_y^2 + \eta_y^{*2}) \quad , \quad (4.19)$$

where we have used the function η_y^* introduced in Eq. (4.2). The contribution to the emittance from the vertical dispersion is¹

$$\epsilon_y = \frac{C_q \gamma^2}{J_y} \frac{\oint |G|^3 \mathcal{H}_y ds}{\oint G^2 ds} \quad (4.20)$$

where $C_q = 55\hbar/(32\sqrt{3}mc) = 3.84 \times 10^{-13}$ meter and J_y is the vertical damping partition. For a ring in the horizontal plane $J_y = 1$; the change in J_y due to errors in the weak coupling limit is negligible.

Since the expected values of $\langle \eta_y^2 \rangle / \beta_y$ and $\langle \eta_y^{*2} \rangle / \beta_y$ are equal and are independent of s , the expected value of the emittance can be written

$$\langle \epsilon_y \rangle = 2 \frac{C_q \gamma^2}{J_y} \frac{\langle \eta_y^2 \rangle}{\beta_y} \frac{\int |G|^3 ds}{\int G^2 ds} = 2J_\epsilon \frac{\langle \eta_y^2 \rangle}{\beta_y} \sigma_\epsilon^2 \quad , \quad (4.21)$$

where, the relative energy spread¹ has been used to simplify the expression and J_ϵ is the longitudinal damping partition. Since J_ϵ is typically between 1 and 2, one can see that the emittance increase has a larger contribution to the beam size than the coupling increase of Eq. (4.18).

At this point, we will again emphasize the distinction between these two effects. As mentioned, the first effect, Eq. (4.18), is due to a coupling between the energy deviation and the vertical position; it does not change the beam's six-dimensional emittance. In contrast, the second effect, Eq. (4.20), causes a fundamental increase in the phase space volume occupied by the beam. In a synchrotron light source this distinction is irrelevant, but in a damping ring it is important because, unlike the first effect, the emittance increase cannot be corrected once the beam has been extracted from the ring. Of course, both effects can be corrected by correcting the vertical dispersion in the ring; this is the subject of Section 6.

4.5 SIMULATIONS

To verify these results, the computer program CEMIT⁸ has been used to simulate various errors in the Stanford Linear Collider (SLC) North Damping Ring (NDR).¹⁵ The NDR is designed to operate on the coupling difference resonance, but for these

simulations the tunes were shifted to $\nu_x = 8.375$ and $\nu_y = 3.275$; this lattice will be referred to as the NDR1. Finally, in this comparison, we will only discuss the increase in the vertical emittance due to the vertical dispersion.

The results of simulating rotational misalignments in the quadrupoles and vertical misalignments in the sextupoles are listed in Table 2. The misalignments were generated from gaussian distributions with an rms of 0.5 mrad and $150\mu\text{m}$, respectively. The calculated values are found using Eqs. (4.7) and (4.21), while the measured values are found by averaging the results from 1000 different random error distributions. Finally, the measured errors are the standard errors of the averaged values. In both cases, one can see that the approximate formula agree well with the simulations.

In addition, Table 2 lists results from simulating the effects of a corrected closed orbit. Here, the results are the average of twenty simulations. The simulations included vertical quadrupole misalignments with an rms of $150\mu\text{m}$ and vertical BPM misalignments, also, with an rms of $150\mu\text{m}$. The resulting orbit was corrected using the twenty vertical dipole correctors in the NDR to minimize the rms of the measured orbit. Before correction, the rms magnitude of the actual orbit was roughly 1.5 mm; the correction reduced this to $140\mu\text{m}$, roughly the accuracy of the BPM alignment. In this case, the calculated result was found from Eqs. (4.8), (4.12), (4.17), and (4.21), although the dominant contribution comes from Eq. (4.17). Again, the calculated estimate agrees well with the average of the simulations. Finally, notice that the contribution from the corrected orbit is less than the contribution due to similar misalignments in the sextupoles; as mentioned, this occurs since the orbit is still correlated over short segments.

To further study the effect of a corrected closed orbit, the average $\overline{\langle \eta_y^2 \rangle} / \beta_y$ has been plotted versus the chromaticity of the ring. In Fig. 1, the closed orbit was not corrected while in Fig. 2 the orbit was corrected with twenty correctors. Again, the data

and errors were found from the results of twenty simulations. The lines are calculated using Eqs. (4.8), (4.11), and (4.15) and Eqs. (4.8), (4.12), and (4.17) for Figs. 1 and 2, respectively.

As one can see, the character of the dispersion changes when the orbit is corrected. In the uncorrected case (Fig. 1) the dispersion has a sharp minimum close to $\xi_y = 0$, while in the corrected case (Fig. 2), the minimum occurs near $\xi_y = -4.5$. We can understand this change in the following manner. The insertion regions in the NDR do not have local chromatic correction; they are compensated with sextupoles in the arcs. When the orbit is corrected, the minimum value of the dispersion occurs, not when the global chromaticity is corrected, but when the local values of ξ and Δ are the smallest. This occurs when the sextupoles are used to locally compensate only the arcs and not both the insertion regions and the arcs.

Thus, when the chromaticity is zero, correcting the orbit will tend to increase the vertical dispersion *relative* to the closed orbit since ξ_{local} and Δ_{local} grow. This is illustrated in Fig. 3; here, the vertical emittance, normalized by the square of the closed orbit, has been plotted versus the number of correctors used to correct the orbit. Notice that, initially, the normalized vertical emittance increases rapidly as the orbit is corrected; it then peaks and slowly decreases. The initial increase occurs when, in Eq. (4.17), the insertion regions are separated from the arcs. Further correction then just subdivides the arcs which has little effect. The line in Fig. 3 is calculated using the estimates for a corrected orbit. Finally, again notice that Fig. 3 is a plot of the vertical emittance *normalized* by the closed orbit; the actual vertical emittance tends to decrease as the orbit is corrected.

Before concluding this section, it is useful to contrast the behavior seen in Fig. 3 with an example from the ALS lattice.¹⁶ The ALS lattice differs from the NDR in that the

ALS has twelve dispersion-free insertion regions rather than just two. Fig. 4 is a plot of the vertical emittance due to quadrupole misalignments versus the number of correctors used to correct the orbit. Here, the emittance contribution continues to increase rapidly with the number of correctors. There are two reasons for this: first the fractional tune in the ALS is lower than in the NDR1, $\nu_y = 8.18$ as compared to $\nu_y = 3.275$, and thus the ALS is more sensitive to errors. Second, as mentioned, the ALS has twelve insertion regions and the chromatic correction is performed in the arcs between these insertions. As the orbit is corrected, this non-local chromatic correction continues to be broken, causing the dispersion to increase relative to the closed orbit.

5. BETATRON COUPLING

In a conservative system, such as a proton storage ring, betatron coupling leads to “beats” where energy is transferred between the two transverse planes. An e^+/e^- storage ring is not a conservative system; the synchrotron radiation provides both a source of noise and damping. Neglecting the vertical dispersion, only the horizontal plane is coupled to the noise source, while both planes are damped. Thus, in an uncoupled ring, only the horizontal emittance is driven. Unfortunately, in the presence of coupling, the eigenvectors of the betatron motion rotate from the x and y axes so that both eigenmodes couple to the noise in the horizontal plane. Thus, in the case of weak coupling, the vertical beam size is determined by both the projection of the “horizontal” emittance in the vertical plane and the contribution to the “vertical” emittance from the noise in the horizontal plane.

Much like the beam size due to the vertical dispersion, we can separate this increase into two contributions, one due to a coupling which increases the projection of the six-dimensional emittance into the vertical plane, and the other due to a fundamental

increase in the vertical emittance. As before, the former effect will be referred to as the “local” contribution since it depends upon the local value of the coupling. In principal, this local coupling can be corrected at one location in the ring with four independent skew quadrupoles; the four magnets can be used to uncouple the one-turn transport matrix at a specified location. Unfortunately, this does not remove the second effect which arises from the “global” coupling; one would need skew quadrupoles next to every bending magnet to completely remove this contribution.

In this section, we will calculate the beam size increase due to both the local and the global coupling. Paralleling the discussion of the vertical dispersion, we will then calculate the effects of random errors and a non-zero closed orbit. Finally, these analytic results will be compared with the results of simulations.

5.1 VERTICAL BEAM SIZE

To calculate the rms vertical beam size due to the linear betatron coupling, we will start from the equations of motion for a single particle, calculate the rms betatron motion, and finally, average over the ensemble of particles to find the rms beam size. Alternately, one could use the Fokker-Planck equation,⁹ but in many ways the more intuitive approach is appealing since it allows one to explicitly see the cause of the various contributions.

We will analyze the motion assuming that the coupling is weak and the vertical motion is much smaller than the horizontal. Thus, we can use the unperturbed horizontal motion to calculate the vertical. The equation for the vertical betatron motion was calculated, for the weak coupling limit, in Section 2:

$$y''_{\beta} - K_1 y_{\beta} = (K_2 y_c - \tilde{K}_1) x_{\beta} \quad , \quad (2.9)$$

where the effects of the synchrotron radiation have been neglected.

We want to calculate the change in y_β . Treating the magnets as delta-functions, the coupling adds a kick $\Delta y' = x_\beta(K_{2y_c} - \tilde{K}_1)\Delta s$ to the vertical motion which is then exponentially damped by the radiation damping process. Thus, we can express the vertical motion as a sum over the kicks $\Delta y'$

$$y_\beta(s) = \int_{-\infty}^s dz g(z) x_\beta(z) e^{(z-s)\alpha_y/c} \left[\sqrt{\beta_y(s)\beta_y(z)} \sin(\psi_y(s) - \psi_y(z)) \right] . \quad (5.1)$$

Here, g is the coupling coefficient $g(z) = (K_{2y_c} - \tilde{K}_1)$, α_y is the vertical damping rate, and c is the speed of light. In addition, the function enclosed in the brackets is the standard R_{12} betatron matrix element which transforms a deflection $\Delta y'$ at z to a position Δy at s .

At this point we need an expression for the x betatron motion. The horizontal betatron motion is driven by energy fluctuations due to the synchrotron radiation; these are coupled to the horizontal plane through the dispersion. When a photon of energy u is radiated, x_β and x'_β change by $\Delta x_\beta = \eta_x u/E_0$ and $\Delta x'_\beta = \eta'_x u/E_0$. For brevity, we will let η'_x , and thus $\Delta x'_\beta$, equal zero in the next two equations, but this assumption will be removed thereafter. In this case, the horizontal betatron motion is just a sum of displacements Δx_β which are exponentially damped:

$$x_\beta(s) = \sum_{\substack{i=-\infty \\ \{photons\}}}^s \xi_i \eta_x(z_i) e^{(z_i-s)\alpha_x/c} \left[\sqrt{\frac{\beta_x(s)}{\beta_x(z_i)}} (\cos \Delta\psi_x + \alpha_x(z_i) \sin \Delta\psi_x) \right] . \quad (5.2)$$

Here, ξ_i is a stochastic variable equal to the relative energy (u/E_0) of a photon radiated at z_i . In addition, $\Delta\psi_x = \psi_x(s) - \psi_x(z_i)$ and the function in brackets is the R_{11} betatron matrix element which transforms a change in position Δx at z_i to a Δx at s .

Now, we can use Eq. (5.2) to express Eq. (5.1) as a sum over photons ξ_i ,

$$y_\beta(s) = \sum_{\substack{i=-\infty \\ \{\text{photons}\}}}^s \xi_i \eta_x(z_i) \int_{z_i}^s dz e^{(z_i-z)\alpha_x/c} R_{11x}(z_i, z) e^{(z-s)\alpha_y/c} g(z) R_{12y}(z, s) \quad . \quad (5.3)$$

The vertical beam size is now found by averaging the equilibrium value of y_β^2/β_y over the ensemble of particles. The calculation simplifies since the radiation is a stochastic process, $\langle \xi_i \xi_j \rangle = \langle \xi_i^2 \rangle \delta_{ij}$. In addition, when performing the ensemble average, we can express the sum over photons as the integral of a rate of emission.¹ Thus,

$$\sum_{\substack{i=-\infty \\ \{\text{photons}\}}}^s \langle u_i^2 \rangle \Rightarrow \int_{-\infty}^s \frac{dz_i}{c} \mathcal{N} \langle u^2(z_i) \rangle \quad , \quad (5.4)$$

where \mathcal{N} is the rate of emission. This yields a beam size of

$$\begin{aligned} \frac{\sigma_y^2(s)}{\beta_y(s)} &= \int_{-\infty}^s \frac{dz_i}{c} \mathcal{N} \frac{\langle u^2(z_i) \rangle}{E_0^2} \left[\int_{z_i}^s dz g(z) e^{(z_i-z)\alpha_x/c} e^{(z-s)\alpha_y/c} \sqrt{\beta_x(z)\beta_y(z)} \sin \Delta\psi_y \right. \\ &\times \left. \left(\frac{\eta_x(z_i)}{\sqrt{\beta_x(z_i)}} (\cos \Delta\psi_x + \alpha_x(z_i) \sin \Delta\psi_x) + \eta'_x(z_i) \sqrt{\beta_x(z_i)} \sin \Delta\psi_x \right) \right]^2 \quad , \end{aligned} \quad (5.5)$$

where $\Delta\psi_x = \psi_x(z) - \psi_x(z_i)$ and $\Delta\psi_y = \psi_y(s) - \psi_y(z)$. Notice that we have included the both the contribution from η_x and η'_x .

To evaluate this, we separate the integral over z into a portion over an integral number of turns of the ring and a portion over the remaining segment. Thus, the result has the form:

$$\int_{-\infty}^s dz_i \left[\int_{z_i}^s dz \cdots \right]^2 \Rightarrow \sum_n \int_{s-C}^s dz_i \left[\sum_j^{n-1} \int_{s-C}^s dz \cdots + \int_{z_i-nC}^{s-nC} dz \cdots \right]^2 \quad , \quad (5.6)$$

where \cdots is used to represent the integrand.

At this point, we assume that the tunes are far from the coupling resonances, $\nu_x \pm \nu_y = n$, and damping per turn is small compared to the tunes, $2\pi(\nu_x \pm \nu_y) \gg \alpha_x T_0, \alpha_y T_0$. Now, we can perform the integral over z_i and the sum over the turns. After some algebra, that is explicitly displayed in Appendix B, we find contributions to the vertical beam size and emittance from both the sum and difference resonances of

$$\frac{\sigma_y^2(s)_{\text{local}}}{\beta_y(s)} = \frac{\epsilon_x}{16} \left[\sum_{\pm} \frac{|Q_{\pm}(s)|^2}{\sin^2 \pi \Delta \nu_{\pm}} - 2 \operatorname{Re} \frac{Q_+(s) Q_-^*(s)}{\sin \pi \Delta \nu_+ \sin \pi \Delta \nu_-} \right] \quad (5.7)$$

$$\epsilon_y = \frac{C_q \gamma^2}{16 J_y \oint G^2 ds} \oint_0^C ds \mathcal{H}_x |G^3| \left[\sum_{\pm} \frac{|Q_{\pm}(s)|^2}{\sin^2 \pi \Delta \nu_{\pm}} + 2 \operatorname{Re} \frac{Q_+(s) Q_-(s)}{\sin \pi \Delta \nu_+ \sin \pi \Delta \nu_-} \right]$$

where

$$Q_{\pm}(s) = \int_s^{s+C} dz g \sqrt{\beta_x \beta_y} e^{i[(\psi_x(s) \pm \psi_y(s)) - (\psi_x(z) \pm \psi_y(z)) + \pi(\nu_x \pm \nu_y)]} \quad (5.8)$$

Here, $g = (K_2 y_c - \tilde{K}_1)$ and the sum over \pm denotes a sum over both the $+$ term (sum resonance) and the $-$ term (difference resonance) while $\Delta \nu_+ = \nu_x + \nu_y$ and $\Delta \nu_- = \nu_x - \nu_y$. In addition, the $*$ is used to represent the complex conjugate and the operator “Re” yields the real portion of the expression.

Equation (5.7) explicitly displays the physics described in the beginning of this section. The first expression represents the projection of the “horizontal” emittance into the vertical plane and the second expressions describes the contribution to the “vertical” emittance from the horizontal dispersion. This is analogous to the situation with the vertical dispersion where the local beam size is increased by the local value of the dispersion while the vertical emittance is increased by the average value of the dispersion.

This analogy can be taken further by noticing that the real part of $Q_{\pm} / \sin \pi \Delta \nu_{\pm}$ is analogous to the vertical dispersion or the vertical closed orbit with a phase advance

of $\psi_x \pm \psi_y$ instead of ψ_y . In addition, the imaginary portion of $Q_{\pm}(s)/\sin \pi \Delta \nu_{\pm}$ is analogous to $\eta_y^*(s)$, Eq. (4.2). Thus, $|Q_{\pm}(s)|^2/\sin^2 \pi \Delta \nu_{\pm}$ is completely analogous to $\mathcal{H}(s)$, defined in Eq. (4.19). This analogy will be used in Section 6 when we discuss correction of the coupling.

At this point, we should compare our result with the results of others. Equation (5.7) is similar to the result found in Ref. 9 where the expression was derived by solving the Fokker-Planck equation when close to the difference coupling resonance. The results differ in that (1) the effect of the sum resonance and the cross terms between the sum and difference resonances have been included, (2) the contribution to the vertical emittance involves the *average* of the coupling coefficient around the ring while the contribution to the local beam size just depends upon the local value of the coupling, and (3) the explicit form of the coupling coefficients differ slightly. In many references, including Refs. 2, 9, 10, and 17, the coupling coefficient is found by Fourier analyzing the coupling and only choosing the coefficient closest to the difference resonance. This is not valid in our case since we have assumed that the ring is far from both coupling resonances.

5.2 RANDOM ERRORS

Now we evaluate Eq. (5.7) for specific errors. The quadrupole rotational errors, sextupole misalignments, and the closed orbit are all independent. Thus, the square of the coupling function g is

$$\langle g(z)g(z') \rangle = 4K_1(z)K_1(z')\langle \Theta\Theta' \rangle + K_2(z)K_2(z')(\langle y_m y_m' \rangle + \langle y_c y_c' \rangle) \quad (5.9)$$

where primes have been used to indicate functions of z' rather than z . In the case of uncorrected coupling, we can quickly evaluate Eq. (5.7) to find the contribution from

random quadrupole rotations and random sextupole misalignments. Specifically, we find expressions similar to those quoted in Ref. 3:

$$\frac{\langle \sigma_y^2 \rangle_{\text{local}}}{\beta_y} = \frac{\epsilon_x (1 - \cos 2\pi\nu_x \cos 2\pi\nu_y)}{4 (\cos 2\pi\nu_x - \cos 2\pi\nu_y)^2} \sum_{\text{quad}} (K_1 L)^2 4\Theta^2 \beta_x \beta_y$$

$$\frac{\langle \sigma_y^2 \rangle_{\text{local}}}{\beta_y} = \frac{\epsilon_x (1 - \cos 2\pi\nu_x \cos 2\pi\nu_y)}{4 (\cos 2\pi\nu_x - \cos 2\pi\nu_y)^2} \sum_{\text{sext}} (K_2 L)^2 y_m^2 \beta_x \beta_y$$
(5.10)

and

$$\langle \epsilon_y \rangle = \frac{\epsilon_x \alpha_x (1 - \cos 2\pi\nu_x \cos 2\pi\nu_y)}{4 \alpha_y (\cos 2\pi\nu_x - \cos 2\pi\nu_y)^2} \sum_{\text{quad}} (K_1 L)^2 4\Theta^2 \beta_x \beta_y$$

$$\langle \epsilon_y \rangle = \frac{\epsilon_x \alpha_x (1 - \cos 2\pi\nu_x \cos 2\pi\nu_y)}{4 \alpha_y (\cos 2\pi\nu_x - \cos 2\pi\nu_y)^2} \sum_{\text{sext}} (K_2 L)^2 y_m^2 \beta_x \beta_y$$
(5.11)

Here, the sum of $1/\sin^2 \pi(\nu_x \pm \nu_y)$ has been written in terms of $\cos 2\pi\nu_x$ and $\cos 2\pi\nu_y$ and we have simplified the expression with the *equilibrium* horizontal emittance.

Finally, notice that the cross terms have not been included in Eq. (5.7). These terms add contributions of

$$\frac{\langle \sigma_y^2 \rangle_{\text{local}}}{\beta_y} = \frac{\epsilon_x \sin 2\pi\nu_y \sum_{\text{quad}} (K_1 L)^2 4\Theta^2 \beta_x \beta_y + \sum_{\text{sext}} (K_2 L)^2 y_m^2 \beta_x \beta_y}{16 \sin \pi \Delta\nu_+ \sin \pi \Delta\nu_-}$$

$$\epsilon_y = \frac{\epsilon_x \alpha_x \sin 2\pi\nu_x \sum_{\text{quad}} (K_1 L)^2 4\Theta^2 \beta_x \beta_y + \sum_{\text{sext}} (K_2 L)^2 y_m^2 \beta_x \beta_y}{16 \alpha_y \sin \pi \Delta\nu_+ \sin \pi \Delta\nu_-}$$
(5.12)

Since these contributions are at least $1/2\pi\nu_{x,y}$ smaller than the contributions from the individual resonances, they will be neglected in all future calculations.

5.3 ORBIT ERRORS

To calculate the effect of a closed orbit, we use Eq. (3.10) or Eqs. (3.7) and (3.9) for the correlation function of a corrected or uncorrected orbit. For an uncorrected orbit, we find

$$\frac{\langle \sigma_y^2 \rangle_{\text{local}}}{\beta_y} \approx \sum_{n, \Delta\nu, \psi_n} \frac{\epsilon_x}{32 \sin^2 \pi \Delta\nu} \frac{\langle y_c^2 \rangle}{\beta_y} c_n \left| \int_s^{s+C} dz K_2(z) \beta_y(z) \sqrt{\beta_x(z)} e^{i\psi_n} \right|^2, \quad (5.13)$$

where the contribution to ϵ_y is similar, but it has as additional coefficient of α_x/α_y and must be averaged over the ring. In addition, the sum over $\Delta\nu$ and ψ_n is a sum over four terms: the two values of $\Delta\nu = \nu_x \pm \nu_y$ and the two values of ψ_n associated with each value for $\Delta\nu$. The values of ψ_n are

$$\psi_n = \psi_x + \begin{cases} (1 + \frac{n}{\nu_y})\psi_y & \text{and} & (1 - \frac{n}{\nu_y})\psi_y, & \Delta\nu = \nu_x + \nu_y \\ -(1 + \frac{n}{\nu_y})\psi_y & \text{and} & -(1 - \frac{n}{\nu_y})\psi_y, & \Delta\nu = \nu_x - \nu_y \end{cases}. \quad (5.14)$$

In the case of a corrected orbit, we find a form similar to Eq. (5.13) except the integral is broken into segments by the correctors

$$\frac{\langle \sigma_y^2 \rangle_{\text{local}}}{\beta_y} \approx \sum_{\Delta\nu, \psi} \frac{\epsilon_x}{32 \sin^2 \pi \Delta\nu} \frac{\langle y_c^2 \rangle}{\beta_y} \sum_{n_c}^{N_{\text{corr}}} \left| \int_{n_c}^{n_c+1} dz K_2(z) \beta_y(z) \sqrt{\beta_x(z)} e^{i\psi} \right|^2 \quad (5.15)$$

where, again, the contribution to ϵ_y is similar. Here, the sum over $\Delta\nu$ and ψ is the same as in the uncorrected case except ψ is now

$$\psi = \begin{cases} \psi_x + 2\psi_y & \text{and} & \psi_x, & \text{if } \Delta\nu = \nu_x + \nu_y \\ \psi_x - 2\psi_y & \text{and} & \psi_x, & \text{if } \Delta\nu = \nu_x - \nu_y \end{cases}. \quad (5.16)$$

The integrals in Eq. (5.15) are the same integrals one finds when using time dependent perturbation theory to calculate the effect of sextupoles on the betatron motion.

The similarity arises because, over a short segment, the closed orbit oscillates like a free betatron oscillation. It is important to emphasize that Eq. (5.15) describes an effect due to linear coupling — notice the resonant denominator in Eq. (5.15); it is not an effect of the third order resonances. Specifically, Eq. (5.15) is only valid when the closed orbit is broken into short segments (by correctors). Notice that if the orbit is broken at every sextupole, Eq. (5.15) reduces to Eq. (5.11) which estimates the effect of random sextupole misalignments. Thus, for comparable orbits and misalignments $y_c \approx y_m$, the contribution to the beam size from the orbit will usually be less than the contribution from the misalignments since the orbit is typically correlated across many sextupoles.

Typically, when correcting the dynamic aperture, one adjusts the sextupole strength and placement so that the first order aberrations will cancel over the ring. For example, in the NDR, the cell phase advances are $\nu_{x \text{ cell}} \approx 0.37$ and $\nu_{y \text{ cell}} \approx 0.12$. This causes the first order geometric aberrations due to the sextupoles to cancel over an arc of roughly 8.5 cells. Unfortunately, when correcting the orbit, we break this cancellation scheme, and thus σ_y^2/β_y normalized by the square of the closed orbit tends to grow.

5.4 SIMULATIONS

To verify the analytic results, the betatron coupling contributions to the vertical emittance were determined from simulations of random alignment errors. Again, the NDR1 lattice was used; this is a lattice of the SLC NDR where the tunes have been changed to $\nu_x = 8.375$ and $\nu_y = 3.275$. Table 3 lists the results of simulating rotational misalignments in quadrupoles and vertical misalignments in sextupoles in the NDR1 lattice. As before, the misalignments are generated from a gaussian distribution with an rms of 0.5 mrad and 150 μm respectively. The calculated values are found using Eq. (5.11). The measured values are found by averaging the result of 1000 different random error distributions and the errors listed are the standard error of the average

of the 1000 simulations; again, there is good agreement between the estimates and the simulation results.

In addition, Table 3 also lists results from simulating the effects of a corrected closed orbit where the results are found from twenty simulations. Here, the simulations included vertical quadrupole misalignments with an rms of $150\mu\text{m}$ and vertical BPM misalignments, also, with an rms of $150\mu\text{m}$. The resulting orbit was corrected using the twenty vertical dipole correctors in the NDR to minimize the rms of the measured orbit. Before correction, the rms magnitude of the actual orbit was roughly 1.5mm ; the correction reduced this to $140\mu\text{m}$. In this case, the calculated result was found from Eq. (5.15). Again, the calculated estimate agrees well with the average of the simulations. Finally, notice that the contribution from the corrected orbit is less than the contribution due to similar misalignments in the sextupoles; as mentioned, this occurs because the orbit is still correlated over short segments.

Finally, in Figs. 5 and 6, the betatron coupling contribution to the vertical emittance, normalized by the square of the closed orbit, is plotted versus the number of orbit correctors used. The points plotted are generated by simulating random quadrupole and BPM misalignments in the NDR and the ALS as was done in Figs. 3 and 4. The line is an approximation of Eq. (5.15) which we evaluated by assuming that correctors were evenly distributed in the ring. Notice that initially the normalized contribution increases roughly linearly with the number of correctors. As mentioned, this occurs since the cancellation is broken by the correctors. Of course, since the residual orbit is decreased by the correction, the actual beam size contribution tends to decrease as the orbit is corrected.

5.5 NON-LINEAR COUPLING EFFECTS

We can also estimate the effects of the higher order coupling resonances. In this case, the equation for the vertical betatron motion is

$$y''_{\beta} + K_1 y_{\beta} = K_p x_{\beta}^m y_{\beta}^n \quad , \quad (5.17)$$

where $p = m + n$. Using perturbation theory, we would find a similar form for the increase in the vertical emittance except that the increase would depend upon higher powers of ϵ_x and the unperturbed vertical emittance. Because ϵ_x and ϵ_y are small, these effects will be negligible unless one is very close to the non-linear coupling resonance. A detailed analysis of these higher order coupling resonances can be found in Ref. 17.

Actually, there is one case where this higher order coupling could be significant. This occurs if the beam is very large when it is injected into the ring. Because of the large beam sizes, the widths of these higher order coupling resonances are larger. In simulations of a future damping ring lattice,¹⁸ coupling has been observed after injecting the beam into the ring which was operating close to the sextupole difference resonance, $\nu_x - 2\nu_y \approx 0.03$. This is actually advantageous in this design since the vertical emittance damps faster when the beams are coupled; this occurs because $J_x = 1.6$ while $J_y = 1.0$ and thus there is more damping in the horizontal plane. Of course, one has to be sure that the beam becomes uncoupled before the horizontal emittance reaches its equilibrium value or the vertical emittance will never damp beyond this point.

6. CORRECTION

In this section, we will discuss reduction and correction of the vertical dispersion and the betatron coupling. The simplest way to reduce these effects is to decrease the sensitivity of the ring to the errors. The most obvious method of doing this is to reduce the resonant denominators $1/\sin^2 \pi\nu_y$ or $1/\sin^2 \pi\Delta\nu_{\pm}$ which appear in all the dispersion and coupling formulas.

In addition to decreasing the sensitivity to the errors, one can correct these effects directly. Specifically, we will first calculate the amount one can correct the vertical dispersion with a pair of correctors, typically skew quadrupoles, separated by ninety degrees in phase. Then, using the analogy between the vertical dispersion and the coupling functions that was noted in Section 5.1, we will apply our results to the correction of the betatron coupling. Finally, we will compare these analytic estimates with the results of simulations.

6.1 VERTICAL DISPERSION

As mentioned, one can also correct the vertical dispersion directly with either skew quadrupoles in regions of horizontal dispersion or orbit bumps in the quadrupoles.¹⁹ Unfortunately, this is complicated because the skew quadrupoles and orbit bumps in the sextupoles also contribute to the betatron coupling. Thus, one has to either compensate the betatron coupling or use orbit bumps in regions without sextupoles; this will effectively limit the number of correctors one can use.

Regardless, the correction of the dispersion itself is relatively simple; the dispersion generated by random errors, much like a closed orbit, will primarily have harmonics near the vertical betatron tune. Thus, as when correcting a close orbit, only a few dispersion correctors are needed to cancel these dominant components, thereby significantly reduc-

ing the dispersion. We will consider two cases: (1) correcting the vertical emittance, *i.e.*, the global effect of the dispersion, and (2) correcting the local dispersion at one location.

6.1.1 Global Correction – Emittance Correction

The vertical emittance due to the dispersion is proportional to the average of $\overline{\mathcal{H}_y}$ in the bend magnets. For this estimate we will assume that this is equal to the average of $\overline{\mathcal{H}_y}$ around the ring. Using a few trigonometric identities, along with Eqs. (4.1), (4.3), and (4.19), we can express \mathcal{H}_y as the squared absolute value of an integral over a complex exponential; this is very similar to the coupling coefficients $|Q_{\pm}|^2 / \sin^2 \pi \Delta \nu_{\pm}$. Thus, the average of \mathcal{H}_y in a ring with two correctors can be written

$$\begin{aligned} \overline{\mathcal{H}_y} = \frac{1}{4 \sin^2 \pi \nu_y} & \left[\overline{\left| \int_s^{s+C} \sqrt{\beta_y(z)} e^{i\psi_y(z)} F(z) dz \right|^2} + a^2 + b^2 \right. \\ & + 2a \operatorname{Re} \overline{\int_s^{s+C} \sqrt{\beta_y(z)} e^{i(2\pi\nu_y - \psi_y(z))} F(z) dz} \\ & \left. - 2b \operatorname{Im} \overline{\int_s^{s+C} \sqrt{\beta_y(z)} e^{i(2\pi\nu_y - \psi_y(z))} F(z) dz} \right] , \end{aligned} \quad (6.1)$$

where the bar is used to denote an average around the ring and a and b are the strengths of the two correctors which are separated by $\pi/2$ in phase and are arbitrarily assumed to be located at $\psi = 0$ and $\psi = -\pi/2$.

To minimize $\overline{\mathcal{H}_y}$, and thereby the emittance, we solve for the a and b which zero the first derivatives of Eq. (6.1). The solutions are

$$\begin{aligned} a &= -\operatorname{Re} \overline{\int_s^{s+C} \sqrt{\beta_y(z)} e^{i(2\pi\nu_y - \psi_y(z))} F(z) dz} \\ b &= +\operatorname{Im} \overline{\int_s^{s+C} \sqrt{\beta_y(z)} e^{i(2\pi\nu_y - \psi_y(z))} F(z) dz} , \end{aligned} \quad (6.2)$$

and these yield a residual dispersion of

$$\overline{\mathcal{H}_y} = \frac{1}{4 \sin^2 \pi \nu_y} \left[\left| \int_s^{s+C} \sqrt{\beta_y(z)} e^{i\psi_y(z)} F(z) dz \right|^2 - a^2 - b^2 \right] . \quad (6.3)$$

Now, we can solve for the expected value due to a distribution of random errors. Assuming that the errors F_i are uniformly distributed in the ring, we find an expected value of

$$\langle \overline{\mathcal{H}_y} \rangle = \frac{1}{6} \sum_i (FL)_i^2 \beta_{yi} , \quad (6.4)$$

where L_i is the length of the element at position i . This result should be compared with the uncorrected expected values, Eqs. (4.7) and (4.19). We see that using two correctors reduces the residual dispersion $\overline{\mathcal{H}_y}$ by a factor of $2/3 \sin^2 \pi \nu_y$.

Strictly, this result is only valid for the vertical dispersion due to uncorrelated errors, but because orbit correction effectively randomizes the orbit, we can also apply the result to the dispersion due to a corrected orbit. Thus, global dispersion correction will reduce the expected values of the beam size and the emittance as

$$\frac{\langle \sigma_y^2 \rangle_{\text{local}}}{\beta_y} = \frac{2}{3} \sin^2 \pi \nu_y \frac{\langle \sigma_y^2 \rangle_0}{\beta_y} \quad \langle \epsilon_y \rangle = \frac{2}{3} \sin^2 \pi \nu_y \langle \epsilon_y \rangle_0 , \quad (6.5)$$

where the subscript 0 is used to denote the values before correction.

Notice that the correction cancels the resonant denominator. We will also find this when we estimate the effect of local correction. The resonant denominator occurs because the vertical dispersion is a periodic function that must close upon itself. When the dispersion is corrected, the boundary conditions are satisfied by the correctors; thus, the resonant denominator no longer appears. This is analogous to correcting the closed orbit or the coupling functions Q_+ and Q_- , which are also periodic functions.

6.1.2 Local Correction

Here, we use the two correctors to zero $\eta_y(s)$ and $\eta'_y(s)$ at one location in the ring; this is equivalent to zeroing $\mathcal{H}_y(s)$. From Eqs. (4.1), (4.2), and (4.3), we find the required corrector strengths

$$\begin{aligned} a &= -\text{Re} \int_s^{s+C} \sqrt{\beta_y(z)} e^{i(2\pi\nu_y - \psi_y(z))} F(z) dz \\ b &= +\text{Im} \int_s^{s+C} \sqrt{\beta_y(z)} e^{i(2\pi\nu_y - \psi_y(z))} F(z) dz \quad , \end{aligned} \quad (6.6)$$

where s is the point that η_y and η'_y are to be corrected to zero. Notice that these solutions are similar to the corrector solutions for global correction; they differ in that the solution for global correction is averaged while this is not.

Now, we need to know how this correction affects the global contribution, *i.e.*, $\overline{\mathcal{H}_y}$. Here, we use Eq. (6.1) with the corrector strengths just calculated. Assuming random errors, we find

$$\langle \overline{\mathcal{H}_y} \rangle = \frac{f_{\text{cor}}}{2} \sum_i (FL)_i^2 \beta_{y_i} \quad , \quad (6.7)$$

which differs from the uncorrected result by a factor of $2f_{\text{cor}} \sin^2 \pi\nu_y$. Here, f_{cor} is a function that depends upon the location of the correctors relative to the location that η_y and η'_y are corrected. In particular,

$$f_{\text{cor}} = \left(1 - \frac{|\Delta\psi_y|}{2\pi\nu_y} \right)^2 \left(\frac{\Delta\psi_y}{2\pi\nu_y} \right)^2 \quad , \quad (6.8)$$

and $\Delta\psi$ is the phase difference from the correctors to the correction. This function varies between one and 1/2, having a minimum when the correctors are separated from the correction point by half the ring and having a maximum when the correctors are immediately adjacent to the correction.

Applying this result, we see that at most positions around the ring,

$$\frac{\langle \sigma_y^2 \rangle_{\text{local}}}{\beta_y} = 2f_{\text{cor}} \sin^2 \pi \nu_y \frac{\langle \sigma_y^2 \rangle_0}{\beta_y} \quad \langle \epsilon_y \rangle = 2f_{\text{cor}} \sin^2 \pi \nu_y \langle \epsilon_y \rangle_0 \quad , \quad (6.9)$$

while at position s : $\langle \sigma_y^2(s) \rangle_{\text{local}} / \beta_y \sim 0$. Finally, notice that after local correction the emittance is between one and a half to three times larger than after global correction, Eq. (6.4); in the worst case, local correction actually increases the global contribution if the fractional tune is greater than 0.25.

6.1.3 Measurement

Of course, to correct the vertical dispersion, one needs to measure it. If the BPMs are sufficiently accurate, one can measure the vertical dispersion directly by changing the beam energy. Alternately, if the BPMs are not sufficiently accurate, one can observe the effects of the vertical dispersion in the beam size. In this case, the vertical emittance is simply minimized with the correction elements. There are two problems with this approach: first, it is hard to decouple the local effect of the dispersion from the increase in the emittance, and second, the finite resolution of the beam size measurement will limit the convergence of the minimization; this will effectively limit the number of correctors that can be used in the minimization procedure.

6.2 BETATRON COUPLING

In this section, we will estimate the amount one can reduce the betatron coupling by directly correcting it with skew quadrupoles or orbit bumps in the sextupoles. In Section 6.1, we calculate the reduction in $\overline{\mathcal{H}_y}$ after both global and local correction using just two correctors. The situation for the betatron coupling is similar, except we need four independent correctors to correct both Q_+ and Q_- .

To perform the calculation correctly, we would need to solve four coupled equations for the skew quadrupole strengths. Instead, we will make use of the analogy, noted in Section 5.1, between Q_{\pm} and the vertical dispersion. This will allow us to use the results of the previous section. Of course, in treating the sum and difference resonance separately, we will neglect the effect of the cross term in Eq. (5.7). This is valid since, as was noted in Section 5, the cross term will tend to be small because of the rapidly oscillating phase. Furthermore, by treating Q_+ and Q_- separately we assume that the correctors for Q_+ do not affect Q_- and vice-versa. Obviously, this is not true of the individual skew quadrupoles, but linear combinations of the four skew quadrupoles will have this property.

6.2.1 Global Correction – Emittance Correction

To estimate the global correction one can perform with four skew quadrupoles, we use the global coupling result of Section 6.1. Thus, global correction will cancel the resonant denominators, reducing the expected values of the emittance and the beam size by $2/3 \sin^2 \pi \Delta \nu_{\pm}$. Specifically, if four skew quadrupoles are used to correct the global coupling contribution, we use Eqs. (5.10) and (5.11) to find an expected residual due to uncorrelated errors of

$$\frac{\langle \sigma_y^2 \rangle_{\text{local}}}{\beta_y} = \frac{\epsilon_x}{12} \left[\sum_{\text{quad}} (K_1 L)^2 4 \Theta^2 \beta_x \beta_y + \sum_{\text{sext}} (K_2 L)^2 y_m^2 \beta_x \beta_y \right] \quad (6.10)$$

$$\langle \epsilon_y \rangle = \frac{\epsilon_x \alpha_x}{12 \alpha_y} \left[\sum_{\text{quad}} (K_1 L)^2 4 \Theta^2 \beta_x \beta_y + \sum_{\text{sext}} (K_2 L)^2 y_m^2 \beta_x \beta_y \right] ,$$

and we use Eq. (5.15) to find the residual due to a corrected closed orbit of

$$\langle \epsilon_y \rangle = \sum_{\Delta \nu, \psi} \frac{\epsilon_x \alpha_x}{48 \alpha_y} \frac{\langle y_c^2 \rangle}{\beta_y} \sum_{n_c}^{N_{\text{corr}}} \int_{n_c}^{n_c+1} \frac{dz_i}{\Delta s} \left| \int_{z_i}^{n_c+1} dz K_2(z) \beta_y(z) \sqrt{\beta_x(z)} e^{i\psi} \right|^2 , \quad (6.11)$$

where Δs is the distance between correctors and the values of ψ are given by Eq. (5.16).

6.2.2 Local Correction

To estimate the effect of local correction at position s , we could use the results derived in Section 6.1 as we did for the global correction. Alternately, we can observe the effect of local correction by returning to Eq. (5.6). When the local coupling is corrected at location s , the first integral within the square brackets is zero; these integrals are equal to $Q_{\pm}(s)$. The remaining term in Eq. (5.6) will cause an emittance contribution of

$$\epsilon_y = \frac{\epsilon_x \alpha_x}{4 \alpha_y} \int_s^{s+C} \frac{dz_i}{C} \sum_{\pm} \left| \int_{z_i}^{s+C} dz g \sqrt{\beta_x \beta_y} e^{i(\psi_x \pm \psi_y)} \right|^2, \quad (6.12)$$

where s is the point of correction. Here, we have neglected the cross coupling terms. In addition, we have ignored the contribution from the correctors themselves. This is equivalent to assuming that the correctors are located just after point s and thus they do not contribute to the integral. To include the correctors, we only need include the factor f_{cor} that was found in Eq. (6.7).

Now, we use Eq. (6.12) to find the emittance after correction of the local coupling with four skew quadrupoles. For random errors we find

$$\langle \epsilon_y \rangle = f_{\text{cor}} \frac{\epsilon_x \alpha_x}{4 \alpha_y} \left[\sum_{\text{quad}} (K_1 L)^2 4 \Theta^2 \beta_x \beta_y + \sum_{\text{sext}} (K_2 L)^2 y_m^2 \beta_x \beta_y \right], \quad (6.13)$$

where f_{cor} is given by Eq. (6.8). Notice that this result is equal to the estimate of local correction found in Eq. (6.7), namely, the correction changes the global coupling by $2f_{\text{cor}} \sin^2 \pi \Delta \nu_{\pm}$. Also notice that this is a factor of three larger than the result after global correction.

Finally, we estimate effect of a corrected orbit after the local coupling has been corrected. Using Eqs. (6.12) and (5.15), we find

$$\langle \epsilon_y \rangle = f_{\text{cor}} \sum_{\Delta \nu, \psi} \frac{\epsilon_x \alpha_x}{16 \alpha_y} \frac{\langle y_c^2 \rangle}{\beta_y} \sum_{n_c}^{N_{\text{corr}}} \int_{n_c}^{n_c+1} \frac{dz_i}{\Delta s} \left| \int_{z_i}^{n_c+1} dz K_2(z) \beta_y(z) \sqrt{\beta_x(z)} e^{i\psi} \right|^2, \quad (6.14)$$

where Δs is the distance between correctors and the values of ψ are given above by Eq. (5.16).

6.2.3 Measurement

Finally, to perform these corrections, one needs to measure the coupling. Unfortunately, when operating a ring far from the coupling resonances, one cannot rely upon the standard technique of putting the ring on the difference resonance and then adjusting skew quadrupoles to make the two measured tunes equal. First, this technique does not correct the coupling due to the sum resonance. Second, the ring is perturbed when making the measurements and thus even the difference resonance will not be fully corrected when the ring is brought back to its nominal tunes.

Instead, the coupling can be measured by analyzing the coherent motion of a kicked beam.^{20,21} This measurement is convenient since one can measure the local value of the coupling all around the ring. Finally, as in the measurement of the dispersion, additional information can be obtained from measurements of the beam size at synchrotron light monitors or, in a damping ring, from the extracted beam.

6.3 SIMULATIONS

Simulations were performed in the NDR to verify these analytic estimates. First, the effect of correcting the global dispersion was simulated in the NDR1 ring. The correction was performed with two orbit bumps separated by roughly ninety degrees. The bumps were located in regions without sextupoles so there was no contribution to the betatron coupling. The results are listed in Table 4. Again, 1000 simulations were used to calculate the effect of the random misalignments and twenty simulations of a corrected closed orbit. Here, the estimates are found from Eq. (6.5) along with Eq. (4.21) and the equations for random errors Eq. (4.7) or the equations for a corrected closed

orbit, Eqs. (4.8), (4.12), and (4.17). Notice that the vertical emittance was decreased by roughly a factor of three. This is in excellent agreement with our estimate.

Next, the effect of correcting the local coupling was simulated. Four skew quadrupoles were used to completely uncouple the beam at the extraction point of the damping ring; two skew quads were located immediately adjacent to the extraction point while the other two were located on the opposite side of the ring. The results are listed in Table 5. Again, 1000 simulations were used to calculate the effect of the random misalignments and twenty simulations of a corrected closed orbit. In this case, the calculated values are found using Eqs. (6.13) and (6.14) with a value $f_{\text{cor}} = 0.75$ since two correctors are adjacent to the point of correction ($f_{\text{cor}} = 1.0$) and two are halfway around to ring from the point of correction ($f_{\text{cor}} = 0.5$). Notice that the vertical emittance due to the errors is roughly a factor of four smaller than before the correction. Again, the simulated results agree well with the calculated values.

Finally, the effect of correcting the global coupling was simulated. This time the four skew quadrupoles were used to minimize the vertical emittance in the damping ring. The results are listed in Table 6. Here, only 100 simulations were used to calculate the effect of the random misalignments and twenty simulations of a corrected closed orbit; the global correction simulations are computation intensive. In this case, the calculated values are found using Eqs. (6.10) and (6.11). Notice that now the vertical emittance due to the errors is roughly a factor of nine smaller than before the correction. Again, the calculated estimates agree with results of the simulations.

7. DISTRIBUTIONS AND TOLERANCES

In Sections 4, 5 and 6, we have calculated the *expected* values of the vertical emittance and the beam size. Naively, one could simply invert these equations to solve for alignment tolerances. But, when specifying tolerances, one should include a “confidence level” (CL); this is the probability that, given the specified tolerances, any specific machine will be less than the design limit. Typically, one wants to specify a large CL so that there is a small probability of exceeding the design limit. In this section, we will calculate the location of the 95% CL as a function of the expected values calculated previously.

Calculating the CL requires a detailed knowledge of the distribution of the values of the emittance and the beam size in an ensemble of machines. It has been shown that the mean square amplitude of the normalized orbit due to random errors with gaussian distributions should have an exponential distribution function.²² Since the equations for the closed orbit are similar to those of the dispersion function and the betatron coupling, the same result applies to the amplitudes of $\mathcal{H}_y(s)$ and $|Q_{\pm}(s)|^2$.

Here, we will consider the effect of averaging $\mathcal{H}_y(s)$ and $|Q_{\pm}(s)|^2$ over s ; the vertical emittance is equal to the average of these functions in the bending magnets. We will first discuss the distribution of the values of the emittance arising from vertical dispersion and betatron coupling due to random errors. Then, we will discuss the distribution of the values of the local contribution to the vertical beam size. Finally, note that, although the discussion is limited to the effect of random misalignment errors, the effect of a corrected closed orbit is similar.

7.1 EMITTANCE DUE TO VERTICAL DISPERSION

The actual distribution function for the values of the vertical emittance due to random errors is a complicated function. Thus, we will derive an approximate form that can be integrated to solve for the location of the 95% CL. We will do this by solving for the moments of the distribution of emittances. The vertical emittance is given by Eq. (4.20). Assuming identical bending magnets, we can express this in the same form as Eq. (6.1):

$$\epsilon_y = \frac{J_\epsilon \sigma_\epsilon^2}{4 \sin^2 \pi \nu_y} \left| \int_s^{s+C} \sqrt{\beta_y(z)} e^{i\psi_y(z)} F(z) dz \right|^2. \quad (7.1)$$

Now, we solve for the moments assuming random errors with gaussian distributions. This yields

$$\begin{aligned} \langle \epsilon_y \rangle &= \mu \\ \langle \epsilon_y^2 \rangle &= 2\mu^2 \left(1 - \frac{1}{3} \sin^2 \pi \nu_y \right) \\ \langle \epsilon_y^3 \rangle &= 6\mu^3 \left(1 - \frac{2}{3} \sin^2 \pi \nu_y + \frac{2}{45} \sin^4 \pi \nu_y \right) \\ \langle \epsilon_y^4 \rangle &\approx 24\mu^4 \left(1 - \sin^2 \pi \nu_y + \frac{1}{3} \sin^4 \pi \nu_y - \frac{2}{15} \sin^6 \pi \nu_y \right), \end{aligned} \quad (7.2)$$

where μ is the expected value of the emittance calculated in Section 4. The first three moments were calculated from Eq. (7.1), while the fourth moment was fit to data from simulations. These are shown in Fig. 7 where the second, third, and fourth moments, normalized by $n!\mu^n$, are plotted.

Notice that the moments only depend upon the first moment μ and the fractional vertical tune. When the vertical tune is close to an integer, the moments have the form $\mu_n = n!\mu^n$. These are the moments of an exponential distribution as noted in Ref. 22. As the fractional tune increases, the moments decrease, implying that the probability of large emittance values is decreased.

We could attempt to construct a distribution directly from these moments, but, instead, we simply notice that these moments are close to those of a modified χ -squared distribution where the number of degrees of freedom is a function of $\sin^2 \pi \nu_y$. In particular, the distribution density is

$$g(\epsilon_y) = \frac{n}{2\mu} \frac{e^{-\epsilon_y n/2\mu}}{\Gamma(\frac{n}{2})} \left(\frac{\epsilon_y n}{2\mu}\right)^{\frac{n}{2}-1}, \quad (7.3)$$

where μ is the expected value of the emittance and n is the number of degrees of freedom which depends upon $\sin^2 \pi \nu_y$:

$$\frac{n}{2} = \frac{1}{1 - \frac{2}{3} \sin^2 \pi \nu_y}. \quad (7.4)$$

With these definitions, this distribution has the same first and second moments as the value of the vertical emittance, Eq. (7.2). Furthermore, when the tune is integral, Eq. (7.3) is the density of an exponential distribution which is equal to the distribution of the emittances. In addition, when the fractional tune increases to 0.5, the third and fourth moments of Eq. (7.3) are within 2% and 8% of the moments of the value of the vertical emittance.

These distributions are illustrated in Fig. 8 where the distribution density of the vertical emittance, arising from random errors, has been plotted for three different tunes. All of the histograms are generated from 1000 simulations of $150\mu\text{m}$ vertical sextupole misalignments in the NDR. In Fig. 8(a), the tune is $\nu_y = 3.07$, while in Figs. 8(b) and 8(c) the tunes are $\nu_y = 3.275$ and $\nu_y = 3.43$. In addition, the approximate distribution density of Eq. (7.3) is plotted for each of these three cases. One can see that there is fairly good agreement between the simulations and the approximation.

Now, we need to calculate the distribution after correction of the vertical dispersion. After global correction, the expected value of the emittance is given by Eq. (6.5). In addition, the second moment of the distribution can be found from Eq. (6.1). It is

$$\langle \epsilon_y^2 \rangle = 2\mu^2 \left(\frac{7}{5} \right) . \quad (7.5)$$

Notice that this second moment is independent of the tune. Thus, we would expect the 95% CL to only be weakly dependent upon the fractional tune. To approximate this distribution, we simply choose n to equate the second moment of Eq. (7.3) with this second moment; this occurs when $n = 5.0$.

The distribution density of the value of the vertical emittance after global correction is illustrated in Fig. 8(d). The data was found from 1000 simulations of random sextupole misalignments in the NDR1 and the approximate distribution is found from Eq. (7.3) where $n = 5.0$. Here, our approximation does not accurately reproduce the distribution density for emittance values less than $2\langle \epsilon_y \rangle$, but it does describe the tail of the distribution well; this is ultimately what we need to know to calculate the location of the 95% CL.

At this point, we can calculate the location of the 95% CL for the distributions. This found by integrating the distribution density

$$\int_0^{f_{\text{CL}}(\epsilon_y)} g(\epsilon_y) d\epsilon_y = 0.95 \quad , \quad (7.6)$$

where f_{CL} is the location of the 95% CL in units of the expected vertical emittance. The results are plotted in Fig. 9 as a function of the fractional vertical tune $\Delta\nu_y$. The solid curve is calculated from Eq. (7.3), while the simulation results are plotted as solid circles. One can see that there is very close agreement between the simulation and the approximation results.

In addition, the value of f_{CL} after global correction of the dispersion has also been plotted in Fig. 9. The simulated data is plotted as open circles while the dashed line is our approximation. Although the agreement between the simulated results and the approximation for the correction is not great, as expected, f_{CL} is only weakly dependent upon the fractional tune and it is usually much less than the f_{CL} of the uncorrected cases.

Finally, it is important to note the following: first, the curves for f_{CL} are universal. The only dependence comes from the fractional vertical tune. The value of f_{CL} is independent of the type of errors, the lattice type, and the integral portion of the tune. The data in Fig. 9 has been compared with simulations run on the ALS:¹⁶ a Triple Bend Achromat lattice with an integral tune of 8, and a future damping ring design:¹⁸ a FODO lattice with an integral tune of 11. In both cases, excellent agreement was found with the curve in Fig. 9.

Second, our calculations have assumed that the errors are random with gaussian distributions. A more realistic error distribution is a gaussian distribution where the tails are cutoff at $\pm 2\sigma$; it is doubtful that large alignment errors, values that are many σ , would go undetected. This will reduce f_{CL} even further, making Fig. 9 a conservative estimate of f_{CL} .

And lastly, notice that there are two advantages of increasing the fractional tune towards a half-integer: the expected value of the emittance decreases *and* the probability of large deviations above this expected value also decreases.

7.2 EMITTANCE DUE TO BETATRON COUPLING

Now, we can use the results of the previous section to calculate the distribution of the value of the vertical emittance arising from betatron coupling. Ignoring the cross term in Eq. (5.7), the emittance is the sum of the two quantities $\overline{|Q_{\pm}|^2}$. As noted earlier, these two values have the same form as $\overline{\mathcal{H}_y}$ and thus they should each have

approximate distributions given by Eq. (7.3). Furthermore, if $\overline{|Q_+|^2}$ and $\overline{|Q_-|^2}$ are mutually independent, then the distribution of their sum is just the convolution of the two individual distributions.

Since we have assumed that the errors have gaussian distributions, Q_+ and Q_- will be independent if²³

$$\begin{aligned} \int_s^{s+C} dz \langle F^2(z) \rangle \beta_x \beta_y e^{i2\psi_x} &= 0 \\ \int_s^{s+C} dz \langle F^2(z) \rangle \beta_x \beta_y e^{i2\psi_y} &= 0 \end{aligned} \quad (7.7)$$

Both of these conditions will be (approximately) satisfied if there are many errors in a betatron period, $N \gg \nu_{x,y}$, and if the tunes are large, $\nu_{x,y} \gg 1$; this is typical of high tune (low emittance) rings.

Convolving the two individual distributions for $\overline{|Q_+|^2}$ and $\overline{|Q_-|^2}$, we find an approximate distribution for the value of the vertical emittance:

$$\begin{aligned} g(\epsilon_y) &= \left(\frac{n_+}{2\mu_+} \right)^{\frac{n_+}{2}} \left(\frac{n_-}{2\mu_-} \right)^{\frac{n_-}{2}} \frac{e^{-\epsilon_y n_- / 2\mu_-}}{\Gamma(\frac{n_+}{2}) \Gamma(\frac{n_-}{2})} \\ &\times \int_0^{\epsilon_y} dx e^{-x(\frac{n_+}{2\mu_+} - \frac{n_-}{2\mu_-})} x^{\frac{n_+}{2}-1} (\epsilon_y - x)^{\frac{n_-}{2}-1} \quad , \end{aligned} \quad (7.8)$$

where n_+ and n_- are

$$\frac{n_{\pm}}{2} = \frac{1}{1 - \frac{2}{3} \sin^2 \pi \Delta \nu_{\pm}} \quad , \quad (7.9)$$

and μ_{\pm} are the expected values of the contributions from the sum and difference resonances; these were found in Section 5. Although the integral in Eq. (7.8) can be expressed in terms of the degenerate hypergeometric function, sometimes called Kummer's function, there is no simple evaluation and thus it is left as is.

The distribution of the emittances is illustrated in Fig. 10 where the distribution density is plotted for two sets of tunes. In Fig. 10(a) the tunes are $\nu_x = 8.375$ and $\nu_y = 3.275$ so that $\Delta\nu_+ = 0.35$ and $\Delta\nu_- = 0.10$, while in Fig. 10(b) the tunes are $\nu_x = 8.425$ and $\nu_y = 2.925$ so that $\Delta\nu_+ = 0.35$ and $\Delta\nu_- = 0.50$. As before the histograms are found from 1000 simulations of random sextupole errors and the curves are calculated from Eq. (7.8). Again, there is very good agreement between the simulations and the approximation.

Now, we can calculate the location of the 95% CL which, in the case of the betatron coupling, is a function of both $\Delta\nu_+$ and $\Delta\nu_-$. This is illustrated in Fig. 11 where f_{CL} is plotted as a function of $\Delta\nu_-$, for $\Delta\nu_+ = 0.35$. The solid circles are the results of simulations and the solid line is calculated from Eq. (7.8). In addition, the f_{CL} , found from 100 simulations of global correction, is plotted for three different tunes; this data is plotted as open circles while the estimated value, found using the approximation of Eq. (7.5), is plotted as a dashed line.

One can see that there is very good agreement between the simulated results and the approximation when $\Delta\nu_-$ is small, but there is a significant discrepancy as $\Delta\nu_-$ increases. In particular, as $\Delta\nu_-$ increases towards the half-integer, the value of f_{CL} seems to depend upon the horizontal and vertical tunes in addition to $\Delta\nu_+$ and $\Delta\nu_-$. For example, when the tunes are $\nu_x = 8.575$ and $\nu_y = 3.075$ ($\Delta\nu_+ = 0.35$ and $\Delta\nu_- = 0.50$), f_{CL} equals 2.05. In contrast, when the tunes are $\nu_x = 8.425$ and $\nu_y = 2.925$ ($\Delta\nu_+ = 0.35$ and $\Delta\nu_- = 0.50$), f_{CL} equals 1.86. Thus, there is a substantial difference in f_{CL} even though $\Delta\nu_{\pm}$ are the same in the two cases. This difference could be explained by the cross term in Eqs. (5.7) and (5.12) which depends upon $\sin 2\pi\nu_x$ along with $\sin \pi\Delta\nu_{\pm}$.

Finally, again notice the following: (1) the curves in Fig. 11 are universal in that all rings will have similar values of f_{CL} , (2) because the actual distributions of errors will

probably not have large value tails, the values of f_{CL} in Fig. 11 are conservative, and (3) there are two advantages of keeping $\Delta\nu_-$ and $\Delta\nu_+$ large: the expected value of the emittance decreases and the probability of large deviations above this expected value also decreases.

7.3 LOCAL BEAM SIZE

Now, we can calculate the distribution of the value of the beam size arising from the local coupling effects. These are simpler than the distributions of the emittances since the contribution depends upon the local value, not the average value, of the coupling. In the case of the dispersion, the beam size σ_y^2/β_y depends upon $\eta_y^2(s)/\beta_y$. As stated, this will have an exponential distribution similar to the closed orbit.²² Thus, the value of the local beam size increase due to dispersion will have an exponential distribution with a 95% CL located at $3.00\langle\sigma_y^2\rangle/\beta_y$; this is equal to the distribution of Eq. (7.3) where $n = 2$ instead of the value specified in Eq. (7.4).

Similarly, the beam size due to local effect of the betatron coupling depends upon both $|Q_-^2(s)|$ and $|Q_+^2(s)|$ which also have exponential distributions. Thus, the resulting distribution can be found from Eq. (7.8) where $n_{\pm} = 2$ instead of the values specified in Eq. (7.9). In this case, we can evaluate the integral in Eq. (7.8), finding

$$g(\langle\sigma_y^2\rangle/\beta_y) = \frac{e^{-\langle\sigma_y^2\rangle/\beta_y\mu_+} - e^{-\langle\sigma_y^2\rangle/\beta_y\mu_-}}{\mu_+ - \mu_-}, \quad (7.10)$$

where μ_{\pm} are the expected contributions for the sum and difference resonances which were found in Section 5. Now, the location of the 95% CL can be calculated directly from this “bi-exponential” distribution. It ranges from $f_{\text{CL}} = 3.00$, when $\mu_+ \gg \mu_-$ or $\mu_- \gg \mu_+$, to $f_{\text{CL}} = 2.37$, when $\mu_+ = \mu_-$.

7.4 TOLERANCES

Finally, one can use the results of this section to calculate tolerances. We have found that the 95% CL occurs at a value between roughly two and three times the expected emittance. To calculate alignment tolerances with a 95% confidence level, we solve for tolerances that yield expected values that are a factor f_{CL} smaller than the design values.

For example, if we wish to limit the vertical emittance due to sextupole misalignments, we can use Eqs. (4.7) and (5.11) along with the appropriate values of f_{CL} to solve for the 95% CL emittance:

$$\epsilon_{y\ 95\%} = \left[\frac{J_\epsilon \sigma_\epsilon^2}{4 \sin^2 \pi \nu_y} \left(\sum_{sext} (K_2 L)^2 \eta_x^2 \beta_y \right) f_{CL\ \eta_y} + \frac{\epsilon_x (1 - \cos 2\pi \nu_x \cos 2\pi \nu_y)}{4 (\cos 2\pi \nu_x - \cos 2\pi \nu_y)^2} \frac{\alpha_x}{\alpha_y} \left(\sum_{sext} (K_2 L)^2 \beta_x \beta_y \right) f_{CL\ \beta} \right] y_m^2, \quad (7.11)$$

where $f_{CL\ \eta_y}$ can be found from Fig. 9 and $f_{CL\ \beta}$ can be found from Fig. 11. It is trivial to invert this to solve for the desired alignment tolerance.

Actually, the factors f_{CL} were calculated for the dispersive contribution and coupling contribution individually. Strictly, to calculate the f_{CL} for the sum of the two contributions requires convolving both distributions. Fortunately, one usually finds that either the dispersive or the coupling contribution dominates and thus the separate values f_{CL} can be used accurately. However, if both contributions are of equal magnitude, this method will result in tolerances that are slightly too severe.

8. SUMMARY

In this paper, we have discussed two of the dominant contributions to the vertical emittance and beam size in e^+/e^- storage rings, namely, the vertical dispersion and the betatron coupling. In addition, we have presented a corrected derivation for the emittance contribution from the opening angle of the synchrotron radiation. Although, this later effect is negligible in the current designs, it does specify a lower bound on the vertical emittance and may be an important limitation in the future.

The vertical dispersion and the betatron coupling are generated by both magnet alignment errors and a non-zero beam trajectory. We have calculated the expected contributions to the vertical emittance and the vertical beam size due to random misalignments of the magnets and a corrected closed orbit. In addition, we have carefully separated the contributions to the vertical emittance and the beam size since local coupling effects can increase the beam size without increasing the emittance. This is important since the emittance is the relevant quantity in some instances while the beam size is in others.

We have also estimated the effectiveness of simple correction techniques in reducing both the vertical emittance and the beam size. In particular, we used one pair of correctors to reduce the vertical dispersion and four skew quadrupoles to reduce the betatron coupling. In general, the correctors reduce the emittance by cancelling the resonant denominators found in the expressions for the emittance due to dispersion or betatron coupling. Of course, two dispersion correctors or four skew quadrupoles cannot be used to zero the respective emittance contributions anymore than two dipole correctors can be used to zero the closed orbit at all locations around a ring.

Finally, we have calculated alignment tolerances to limit the vertical emittance and beam size from the vertical dispersion and the betatron coupling. In particular, we

have calculated approximate distribution functions for the values of the emittance and beam size in an ensemble of machines. From these distributions, we found tolerances that limit the vertical emittance and beam size with a 95% confidence level. In general, these are a factor of $\sqrt{2}$ to $\sqrt{3}$ more severe than tolerances simply calculated from the expected values of the emittance and beam size. It is thought that this analysis could greatly simplify the calculation of alignment tolerances to limit the vertical emittance and beam size, thereby reducing the need for extensive simulation.

ACKNOWLEDGEMENTS

I would like to thank Ron Ruth for many useful discussions during the course of this work.

APPENDIX A

OPENING ANGLE EMITTANCE CONTRIBUTION

In this appendix, we derive the emittance contribution due to the opening angle of the synchrotron radiation. Photons are radiated with an rms angle of $1/\gamma$ relative to the particle trajectory, thereby changing both the longitudinal and transverse momentum of the particle. In a storage ring built in the horizontal plane, the horizontal motion is coupled to the longitudinal via the “dispersion” function, *i.e.* because the horizontal closed orbit is dependant upon the longitudinal momentum. In the horizontal plane, the effect of this coupling dominates the contribution due to the opening angle of the radiation. In contrast, the vertical closed orbit in an ideal machine does not depend upon the longitudinal momentum and thus the radiation opening angle should determine the vertical emittance. In practice, errors in the machine will generate vertical dispersion and couple the horizontal and vertical betatron motion. These effects will then determine the vertical emittance. Still, the emittance due to the opening angle is useful since it specifies a lower bound on the vertical emittance, a lower bound that will be approached by future generation machines.

The emittance contribution due to the opening angle is estimated in Ref. 1 by ignoring the correlation between the energy and angle of the radiated photons. In this approximation, one finds

$$\epsilon_y \simeq \frac{C_q}{2J_y} \frac{\oint \beta_y(s) |G^3(s)| ds}{\oint G^2(s) ds} \quad (\text{A.1})$$

where $C_q = 3.84 \times 10^{-13} \text{m}$, β_y is the vertical betatron function, and $G(s)$ is the bending function: $G(s) = 1/\rho$ where ρ is the instantaneous bending radius. Our derivation will parallel that of Ref. 1, except that the correlation between the energy and angle of the photon will be included. The high energy photons should be radiated at smaller angles than the low energy photons and thus the correct result will be smaller than Eq. (A.1).

When a particle radiates a photon of energy u , the transverse momentum changes

$$\Delta y' = \frac{u}{E_0} \Theta_y \quad \Delta y = 0 \quad . \quad (\text{A.2})$$

where Θ_y is the angle of inclination between the particle trajectory and the path of the photon. The change in y' changes the particle's transverse invariant J ; where J is equal to¹³

$$2J = \gamma y^2 + 2\alpha y y' + \beta y'^2 \quad . \quad (\text{A.3})$$

The change in J is

$$\Delta J = \alpha y \Delta y' + \beta y' \Delta y' + \frac{\beta}{2} (\Delta y')^2 \quad . \quad (\text{A.4})$$

The beam emittance is calculated from J by averaging over an ensemble of particles. Since changes in y' are statistically independent, the change in the emittance is found from the ensemble average of ΔJ . Furthermore, the ensemble averages of y and y' are zero and thus if we assume that the probability of radiation is uncorrelated with the particle position and transverse momentum, then the change in the emittance between position s and $s + ds$ is

$$d\epsilon(s) = \frac{\beta}{2} \overline{\Delta y'^2(s)} \frac{ds}{c} \quad (\text{A.5})$$

where

$$\overline{\Delta y'^2(s)} = \int \frac{u^2 \Theta_y^2}{E_0^2} n(u, \Omega, s) du d\Omega \quad . \quad (\text{A.6})$$

Here, $n(u, \Omega, s) du d\Omega$ is the probable number of photons, with an energy between u and $u + du$ and a solid angle of Ω to $\Omega + d\Omega$, radiated per unit time at position s .

By assuming that $\langle y \Delta y' \rangle = \langle y \rangle \langle \Delta y' \rangle = 0$, as we did in Eq. (A.5), we are ignoring the effect of gradients in the magnets. When the magnetic field has a gradient, the

probability of radiation depends upon the particle position. But, the magnetic field variation across a beam is typically very small and thus we can ignore it. For example, a damping ring design for the NLC¹⁸ has gradients of 300 KG/meter in the 13.1 KG bending magnets while the beam sigma is 4 microns. Thus, the field varies by only 2 Gauss vertically across the beam.

Now, to find the change in the emittance over one turn, we integrate $d\epsilon$ over the ring

$$\Delta\epsilon = \oint \frac{\beta}{2} \frac{\overline{\Delta y'^2} ds}{c} \quad . \quad (\text{A.7})$$

The equilibrium emittance is then calculated by setting the change due to quantum excitation equal to the change due to damping. Thus

$$\epsilon_y = \frac{\tau_y}{4T_0} \oint \frac{ds}{c} \beta_y(s) \int \frac{u^2 \Theta_y^2}{E_0^2} n(u, \Omega, s) du d\Omega \quad (\text{A.8})$$

where τ_y is the vertical damping time and T_0 is the revolution period of the ring. Note that the vertical *emittance* damping rate is $2/\tau_y$.

Thus, we need to evaluate the integral in Eq. (A.8) over u and Ω . The rate of photons emitted with energy between u and $u + du$ multiplied by the energy u is equal to the power radiated with a frequency between $\omega = u/\hbar$ and $(u + du)/\hbar$.

$$un(u, \Omega, s) du d\Omega = \frac{\partial^2 P(u/\hbar, \Omega, s)}{\partial \omega \partial \Omega} d\omega d\Omega \quad (\text{A.9})$$

The classical relation for the differential power radiated by an ultra-relativistic electron in instantaneous circular motion was calculated by Schwinger²⁴

$$\frac{d^2 P(\omega, \psi, s)}{d\omega d\psi} = \frac{e^2}{3\pi^2 c^2} \rho(s) \omega^2 \left(\frac{1}{\gamma^2} + \psi^2 \right)^2 \left[K_{\frac{2}{3}}^2(\xi) + \frac{\psi^2}{1/\gamma^2 + \psi^2} K_{\frac{1}{3}}^2(\xi) \right] \quad (\text{A.10})$$

where

$$\xi \equiv \frac{\omega\rho}{3c} \left(\frac{1}{\gamma^2} + \psi^2 \right)^{\frac{3}{2}} . \quad (\text{A.11})$$

Here, ψ is the angle of inclination above the orbital plane; thus, ψ is equivalent to Θ_y of Eq. (A.2). In addition, $\rho(s)$ is the instantaneous radius of curvature, and $K_{\frac{1}{3}}$ and $K_{\frac{2}{3}}$ are modified Bessel functions. Notice that the azimuthal angle has been integrated out of Eq. (A.10); it would be needed if we wanted to calculate the opening angle contribution to the horizontal emittance, but, as was mentioned earlier, the horizontal emittance is dominated by the dispersive effects.

Thus, the emittance is

$$\epsilon_y = \frac{\tau_y}{4T_0} \frac{27}{\pi^2} \frac{ce^2\hbar}{E_0^2} \oint ds \frac{\beta_y}{|\rho^3|} \int_{-\frac{\pi}{2}}^{\frac{\pi}{2}} d\psi \psi^2 \left(\frac{1}{\gamma^2} + \psi^2 \right)^{-4} \times \quad (\text{A.12})$$

$$\int_0^\infty d\xi \xi^3 \left[K_{\frac{2}{3}}^2(\xi) + \frac{\psi^2}{1/\gamma^2 + \psi^2} K_{\frac{1}{3}}^2(\xi) \right]$$

where ω has been written in terms of ξ . Furthermore, since the integrand is very small for $\psi \sim \pi/2 \gg 1/\gamma$, and decreases rapidly with ψ , we can extend the limits of integration from $\pm\pi/2$ to $\pm\infty$

$$\epsilon_y = \frac{\tau_y}{4T_0} \frac{27}{\pi^2} \frac{ce^2\hbar}{E_0^2} \oint ds \frac{\beta_y}{|\rho^3|} \int_{-\infty}^{\infty} d\psi \psi^2 \left(\frac{1}{\gamma^2} + \psi^2 \right)^{-4} \left[I_{3(\frac{2}{3})} + \frac{\psi^2}{1/\gamma^2 + \psi^2} I_{3(\frac{1}{3})} \right] \quad (\text{A.13})$$

where

$$I_n(\nu) \equiv \int_0^\infty d\xi \xi^n K_\nu^2(\xi) . \quad (\text{A.14})$$

The integral $I_n(\nu)$ is equal to²⁵

$$I_n(\nu) = \frac{1}{4} \frac{\Gamma(\frac{1}{2})\Gamma(\frac{n+1}{2})}{\Gamma(\frac{n}{2}+1)} \Gamma\left(\frac{n+1}{2} + \nu\right) \Gamma\left(\frac{n+1}{2} - \nu\right) , \quad (\text{A.15})$$

where $\Gamma(x)$ is the gamma function. Specifically,

$$I_3(\nu) = \frac{1}{3} \frac{\nu\pi}{\sin \pi\nu} (1 - \nu^2) \quad . \quad (\text{A.16})$$

Next, the integral over ψ is performed using the algebraic integral²⁶

$$\int_0^\infty \frac{x^{2m} dx}{(x^2 + c)^n} = \frac{(2m-1)!!(2n-2m-3)!!\pi}{2(2n-2)!!c^{n-m-1}\sqrt{c}} \quad . \quad (\text{A.17})$$

Finally, substituting for τ_y ,¹ we find for the opening angle contribution to the emittance,

$$\epsilon_y = \frac{13 C_q}{55 J_y} \frac{\oint \beta_y(s) |G^3(s)| ds}{\oint G^2(s) ds} \quad . \quad (\text{A.18})$$

This is a factor of 2.1 times smaller than the estimate in Eq. (A.1). This expression can be further simplified by using the average value of β_y and the rms energy spread. We find

$$\gamma\epsilon_y \approx 0.24 J_\epsilon \overline{\beta_y} \frac{\sigma_\epsilon^2}{\gamma} \quad , \quad (\text{A.19})$$

where $\gamma\epsilon$ is the normalized emittance and J_ϵ and σ_ϵ are the longitudinal damping partition number and the rms energy spread.

Equation (A.18) has been used to calculate the minimum vertical emittance of a future damping ring design:¹⁸

$$\gamma\epsilon_{y \text{ opening angle}} \simeq 6 \times 10^{-10} \text{m-rad} \quad . \quad (\text{A.20})$$

This is a factor of 45 smaller than the specified vertical emittance of $\gamma\epsilon_y \leq 2.7 \times 10^{-8} \text{m-rad}$.

APPENDIX B

COUPLING DERIVATION

In this appendix, we will derive Eqs. (5.7) and (6.12) from Eq. (5.5). We will only explicitly calculate the contributions from the individual coupling resonances; these come from the $\cos(\psi_x(z) - \psi_x(z')) \cos(\psi_y(z) - \psi_y(z'))$ term which is found when one expands the trigonometric functions in Eq. (5.5). The derivation of the cross term is similar except one needs to include all of the trigonometric functions; this is easily accomplished using exponential notation, but, because of the large number of terms, the calculation is quite tedious.

First, we expand the square of the bracket in Eq. (5.5), keeping only the terms:

$$\frac{\mathcal{N}\langle u^2 \rangle \mathcal{H}_x(z_i)}{4E_0^2} \int_{z_i}^s \int dz dz' g(z)g(z') \cdots \cos(\psi_y(z) - \psi_y(z')) \cos(\psi_x(z) - \psi_x(z')) \quad , \quad (\text{B.1})$$

where trigonometric identities have been used in the expansion and only terms depending upon the differences of the phases $\psi(z)$ and $\psi(z')$ were kept. Now, we can use additional trigonometric identities to express this result as

$$\begin{aligned} \frac{\sigma_y^2(s)}{\beta_y} = \int_{-\infty}^s dz_i \frac{\mathcal{N}\langle u^2 \rangle \mathcal{H}_x}{8cE_0^2} \sum_{\pm} \left[\left(\int_{z_i}^s dz e^{(z_i-z)\alpha_x/c + (z-s)\alpha_y/c} \sqrt{\beta_x \beta_y} g \cos(\psi_x \pm \psi_y) \right)^2 \right. \\ \left. + \left(\int_{z_i}^s dz e^{(z_i-z)\alpha_x/c + (z-s)\alpha_y/c} \sqrt{\beta_x \beta_y} g \sin(\psi_x \pm \psi_y) \right)^2 \right] \end{aligned} \quad (\text{B.2})$$

where the sum over \pm represents a sum over the $\psi_x + \psi_y$ phase and the $\psi_x - \psi_y$ phase.

Next, we can condense this into a single integral using a complex exponential. Expressing this in the form of Eq. (5.6), we find

$$\begin{aligned} \frac{\sigma_y^2(s)}{\beta_y} = & \sum_{n=0}^{\infty} \int_{s-C}^s dz_i \frac{\mathcal{N}\langle u^2 \rangle \mathcal{H}_x(z_i)}{8cE_0^2} \sum_{\pm} \left| e^{-n\alpha_x T_0} \sum_{j=0}^{n-1} e^{j(\alpha_x - \alpha_y)T_0 - ij2\pi\Delta\nu} \int_{s-C}^s q_{\pm}(z) dz \right. \\ & \left. + e^{-n\alpha_y T_0 - in2\pi\Delta\nu} \int_{z_i}^s q_{\pm}(z) dz \right|^2 \end{aligned} \quad (\text{B.3})$$

where

$$q_{\pm}(z) = \sqrt{\beta_x \beta_y} g e^{i(\psi_x \pm \psi_x)}. \quad (\text{B.4})$$

In addition, $\Delta\nu = (\nu_x \pm \nu_y)$, T_0 is the revolution time, and it was assumed that the damping per revolution is small compared to the betatron tunes.

Now, we perform the sum over j . The expression within the absolute value signs becomes

$$\begin{aligned} & \left| \frac{ie^{i\pi\Delta\nu}}{2\sin\pi\Delta\nu} \left(e^{-n\alpha_y T_0 - in2\pi\Delta\nu} - e^{-n\alpha_x T_0} \right) \int_{s-C}^s q_{\pm}(z) dz \right. \\ & \left. + e^{-n\alpha_y T_0 - in2\pi\Delta\nu} \int_{z_i}^s q_{\pm}(z) dz \right|^2 \end{aligned} \quad (\text{B.5})$$

At this point, we can calculate the case where the local coupling is zero at location s . When the local coupling is zero, the first integral over q is zero and we are left with only the second term. Thus,

$$\frac{\sigma_y^2(s)_{\text{global}}}{\beta_y} = \sum_{n=0}^{\infty} e^{-2n\alpha_y T_0} \int_{s-C}^s dz_i \frac{\mathcal{N}\langle u^2 \rangle \mathcal{H}_x(z_i)}{8cE_0^2} \sum_{\pm} \left| \int_{z_i}^s q_{\pm}(z) dz \right|^2. \quad (\text{B.6})$$

Now, we perform the final summation, shifting $s \rightarrow s+C$, and assuming that the photons are radiated uniformly around the ring, this yields Eq. (6.12).

If the local coupling is not zero, we can group the terms in Eq. (B.5) as

$$\left| -e^{-n\alpha_x T_0} \left(\frac{ie^{i\pi\Delta\nu}}{2\sin\pi\Delta\nu} \int_{s-C}^s q_{\pm}(z) dz \right) + e^{-n\alpha_y T_0 - in2\pi\Delta\nu} \left(\frac{ie^{i\pi\Delta\nu}}{2\sin\pi\Delta\nu} \int_{s-C}^s q_{\pm}(z) dz + \int_{z_i}^s q_{\pm}(z) dz \right) \right|^2 . \quad (\text{B.7})$$

When the absolute value sign is calculated, the cross term will have an oscillatory term due to the complex exponential. Assuming that $2\pi\Delta\nu_{\pm} \gg \alpha T_0$, this cross term will go to zero when the final sum over n is performed. Thus, we are left with the separate absolute values of the two terms in Eq. (B.7). The first term is simple; the absolute value is

$$\frac{e^{-2n\alpha_x T_0}}{4\sin^2\pi\Delta\nu} \left| \int_s^{s+C} q_{\pm}(z) dz \right|^2 . \quad (\text{B.8})$$

After performing the final sum over n and substituting expression for the emittance, this yields the first expression in Eq. (5.7).

Finally, we have the second term of Eq. (B.7). Let us express this as

$$\frac{e^{-2n\alpha_y T_0}}{4\sin^2\pi\Delta\nu} \left| \left(ie^{i\pi\Delta\nu} + 2\sin\pi\Delta\nu \right) \int_{z_i}^s q_{\pm}(z) dz + ie^{i\pi\Delta\nu} \int_{s-C}^{z_i} q_{\pm}(z) dz \right|^2 . \quad (\text{B.9})$$

Next, we express the sine in exponential form and shift the second integral by C . When we shift the limits by C , we have to include a phase shift of $e^{i2\pi\Delta\nu}$. Thus, Eq. (B.9) becomes

$$\frac{e^{-2n\alpha_y T_0}}{4\sin^2\pi\Delta\nu} \left| ie^{-i\pi\Delta\nu} \int_{z_i}^s q_{\pm}(z) dz + ie^{-i\pi\Delta\nu} \int_s^{z_i+C} q_{\pm}(z) dz \right|^2 . \quad (\text{B.10})$$

Now, we add these two integrals and perform the final summation over n ; this yields the second expression in Eq. (5.7).

If the local coupling is not zero, we can group the terms in Eq. (B.5) as

$$\begin{aligned} & \left| -e^{-n\alpha_x T_0} \left(\frac{ie^{i\pi\Delta\nu}}{2\sin\pi\Delta\nu} \int_{s-C}^s q_{\pm}(z) dz \right) \right. \\ & \left. + e^{-n\alpha_y T_0 - in2\pi\Delta\nu} \left(\frac{ie^{i\pi\Delta\nu}}{2\sin\pi\Delta\nu} \int_{s-C}^s q_{\pm}(z) dz + \int_{z_i}^s q_{\pm}(z) dz \right) \right|^2 . \end{aligned} \quad (\text{B.11})$$

When the absolute value sign is calculated, the cross term will have an oscillatory term due to the complex exponential. Assuming that $2\pi\Delta\nu_{\pm} \gg \alpha T_0$, this cross term will go to zero when the final sum over n is performed. Thus, we are left with the separate absolute values of the two terms in Eq. (B.11). The first term is simple; the absolute value is

$$\frac{e^{-2n\alpha_x T_0}}{4\sin^2\pi\Delta\nu} \left| \int_s^{s+C} q_{\pm}(z) dz \right|^2 . \quad (\text{B.12})$$

After perform the final sum over n , this will be the first expression in Eq. (5.7).

Finally, we have the second term of Eq. (B.11). Let us express this as

$$\frac{e^{-2n\alpha_y T_0}}{4\sin^2\pi\Delta\nu} \left| \left(ie^{i\pi\Delta\nu} + 2\sin\pi\Delta\nu \right) \int_{z_i}^s q_{\pm}(z) dz + ie^{i\pi\Delta\nu} \int_{s-C}^{z_i} q_{\pm}(z) dz \right|^2 . \quad (\text{B.13})$$

Next, express the sine in exponential form and shift the second integral by C . When we shift the limits by C , we have to include a phase shift of $e^{i2\pi\Delta\nu}$. Thus, Eq. (B.13) becomes

$$\frac{e^{-2n\alpha_y T_0}}{4\sin^2\pi\Delta\nu} \left| ie^{-i\pi\Delta\nu} \int_{z_i}^s q_{\pm}(z) dz + ie^{-i\pi\Delta\nu} \int_s^{z_i+C} q_{\pm}(z) dz \right|^2 . \quad (\text{B.14})$$

Now, we add these two integrals and perform the final summation over n ; this yields the second expression in Eq. (5.7).

REFERENCES

1. M. Sands, "The Physics of Electron Storage Rings," SLAC-121 (1971).
2. A. W. Chao, M. J. Lee, "Vertical Beam Size due to Orbit and Alignment Errors," SLAC-PUB-1915 (1977).
3. A. Piwinski, "Beam Height in PETRA," DESY M-83-19 (1983).
4. T. Suzuki, "Vertical Dispersion Produced by Random Closed Orbit Distortions and Sextupoles," PEP-259 (1977).
5. J. Kewisch, T. Limberg, J. Rossbach, F. Willeke, "Vertical Dispersion Generated by Correlated Closed Orbit Deviations," DESY 86-020 (1986).
6. A. W. Chao, "Evaluation of Beam Distribution Parameters in an Electron Storage Ring," *J. Appl. Phy.*, **50**, 595 (1979).
7. F. Willeke, G. Ripken, "Methods of Beam Optics," *AIP Conf. Proc. 184: Proc. of the 1987 US Part. Acc. School*, AIP, New York, 1989, p. 758.
8. T. O. Raubenheimer, "A Formalism and Computer Program for Coupled Lattices," *Proceedings of the 1989 IEEE Part. Acc. Conf.*, Chicago IL., p. 1313.
9. A. W. Chao, M. J. Lee, "Particle Distribution Parameters in an Electron Storage Ring," *J. App. Phys.*, **47** 4453 (1976).
10. G. Guignard, "Linear Coupling in Storage Rings with Radiating Particles," CERN ISR-BOM/79-30 (1979).
11. G. Guignard, "Betatron Coupling with Radiation," *Proc. of the 1985 CERN Advanced Acc. School*, CERN 87-03 (1987), p. 203.
12. Many laboratories are designing damping rings for future linear colliders that have vertical emittances of $\epsilon_y \sim 1 \times 10^{-11}$ m-rad. Details of the SLAC design can be

found in Ref. 16. Other preliminary designs can be found in:

Proc. of the Int. Work. on Next-Generation Lin. Coll., SLAC-Report-335 (1988).

13. R. D. Ruth, "Single Particle Dynamics in Circular Accelerators," *AIP Conf. Proc. 153: Proc. of the 1985 US Part. Acc. School*, AIP, New York, 1987, p. 150.
14. E.D. Courant, H.S. Snyder, "Theory of the Alternating-Gradient Synchrotron," *Annals of Phys.*, **3**, 1 (1958).
15. The SLC Design Handbook, R. Erickson Ed., SLAC, Stanford CA (1986).
16. The ALS is a 1-2 GeV synchrotron light source.
1-2 GeV Synchrotron Radiation Source: Conceptual Design Report, LBL-PUB-5172 Rev. (1986).
17. G. Guignard, "The General Theory of All Sum and Difference Resonances in a Three-Dimensional Magnetic Field in a Synchrotron, Parts I and II," CERN ISR-MA/75-23 and CERN ISR-MA/75-35 (1975).
18. T. O. Raubenheimer, L. Z. Rivkin, and R. D. Ruth, "Damping Ring Designs for a TeV Linear Collider," SLAC-PUB-4808 (1988) and *Proceedings of the DPF Summer Study, Snowmass '88*, Snowmass CO.
T. O. Raubenheimer, *et al.*, "A Damping Ring Design for Future Linear Colliders," *Proc. of the 1989 IEEE Part. Acc. Conf.*, Chicago IL., p. 1316.
19. E. Close, *et. al.*, "A Proposed Orbit and Vertical Dispersion Correction System for PEP," PEP-271 (1978).
20. J. Bengtsson, "Non-Linear Transverse Dynamics for Storage Rings with Applications to the Low-Energy Antiproton Ring (LEAR) at CERN," CERN 88-05, Ph.D. Thesis (1988).

21. P. P. Bagley and D. L. Rubin, "Correction of Transverse Coupling in a Storage Ring," *Proc. of the 1989 IEEE Part. Acc. Conf.*, Chicago IL., p. 874.
P. P. Bagley, Ph.D. Thesis in preparation.
22. G. Lüders, *Nuovo Cimento Suppl.*, **2**, 1075 (1955).
23. This is a property of sums of gaussian random variables. For example see:
M. Fisz, "Probability Theory and Mathematical Statistics - Third Edition," Wiley, New York (1963), p. 150.
24. J. Schwinger, "On the Classical Radiation of Accelerated Electrons," *Phy. Rev.*, **75**, 1912 (1949).
25. I. S. Gradshteyn and I. M. Ryzhik, "Tables of Integrals, Series, and Products," Academic Press, Orlando FL (1980). Integral 6.576.4.
26. I. M. Gradshteyn and I. M. Ryzhik, *ibid.* Integral 3.251.5.

11. TABLES

Table 1. Effects of rotational [Θ] and vertical [y_m] misalignments.

Misalignment	Effect	Result
Vert. BPM	$y_c \approx y_m$	non-zero closed orbit
Vert. Quad.	$\Delta G_x = -K_1 y_m$	dipole kick
Vert. Sext.	$\Delta \tilde{K}_1 = K_2 y_m$	coupling
Rot. Bend	$\Delta G_x = -G\Theta$	dipole kick
Rot. Quad.	$\Delta \tilde{K}_1 = 2K_1\Theta$	coupling

Table 2. ϵ_y from vertical dispersion due to misalignments in the NDR1.

Misalignment	Calc. ϵ_y	Simulated ϵ_y
Random quad. $\Theta = 0.5$ mrad	1.91×10^{-12}	$1.83 \pm 0.05 \times 10^{-12}$
Random sext. $y_m = 150\mu\text{m}$	6.51×10^{-12}	$6.42 \pm 0.16 \times 10^{-12}$
Corrected closed orbit due to random quad. $y_m = 150\mu\text{m}$ and BPM $y_m = 150\mu\text{m}$	1.32×10^{-12}	$1.1 \pm 0.2 \times 10^{-12}$

Table 3. ϵ_y from betatron coupling due to misalignments in the NDR1.

Misalignment	Calc. ϵ_y	Simulated ϵ_y
Random quad. $\Theta = 0.5$ mrad	6.00×10^{-12}	$6.17 \pm 0.14 \times 10^{-12}$
Random sext. $y_m = 150\mu\text{m}$	1.16×10^{-11}	$1.11 \pm 0.02 \times 10^{-11}$
Corrected closed orbit due to random quad. $y_m = 150\mu\text{m}$ and BPM $y_m = 150\mu\text{m}$	2.01×10^{-12}	$2.6 \pm 0.3 \times 10^{-12}$

Table 4. ϵ_y from globally corrected vertical dispersion in the NDR1.

Misalignment	Calc. ϵ_y	Simulated ϵ_y
Random quad. $\Theta = 0.5$ mrad	0.72×10^{-12}	$0.80 \pm 0.02 \times 10^{-12}$
Random sext. $y_m = 150\mu\text{m}$	2.44×10^{-12}	$2.35 \pm 0.04 \times 10^{-12}$
Corrected closed orbit due to random quad. $y_m = 150\mu\text{m}$ and BPM $y_m = 150\mu\text{m}$	0.50×10^{-12}	$0.60 \pm 0.02 \times 10^{-12}$

Table 5. ϵ_y from locally corrected coupling due to misalignments in the NDR1.

Misalignment	Calc. ϵ_y	Simulated ϵ_y
Random quad. $\Theta = 0.5$ mrad	1.52×10^{-12}	$1.69 \pm 0.03 \times 10^{-12}$
Random sext. $y_m = 150\mu\text{m}$	3.00×10^{-12}	$3.36 \pm 0.06 \times 10^{-12}$
Corrected closed orbit due to random quad. $y_m = 150\mu\text{m}$ and BPM $y_m = 150\mu\text{m}$	1.01×10^{-12}	$1.7 \pm 0.2 \times 10^{-12}$

Table 6. ϵ_y from globally corrected coupling due to misalignments in the NDR1.

Misalignment	Calc. ϵ_y	Simulated ϵ_y
Random quad. $\Theta = 0.5$ mrad	0.68×10^{-12}	$0.71 \pm 0.08 \times 10^{-12}$
Random sext. $y_m = 150\mu\text{m}$	1.33×10^{-12}	$1.55 \pm 0.09 \times 10^{-12}$
Corrected closed orbit due to random quad. $y_m = 150\mu\text{m}$ and BPM $y_m = 150\mu\text{m}$	0.44×10^{-12}	$0.7 \pm 0.1 \times 10^{-12}$

12. FIGURE CAPTIONS

Fig. 1. The average of η_y^2/β_y vs. ξ_y for an uncorrected closed orbit. Data points are calculated from 20 simulations while the curve is found from the analytic results.

Fig. 2. The average of η_y^2/β_y vs. ξ_y for a closed orbit corrected with 20 correctors. Data points are calculated from 20 simulations while the curve is found from the analytic results.

Fig. 3. ϵ_y/y_c^2 due to vertical dispersion vs. N_{corr} in the NDR1 lattice. Data points are calculated from 20 simulations while the curve is found from the analytic results.

Fig. 4. ϵ_y/y_c^2 due to vertical dispersion vs. N_{corr} in the ALS.

Fig. 5. ϵ_y/y_c^2 due to linear coupling vs. N_{corr} in the NDR1 lattice. Data points are calculated from 20 simulations while the curve is found from the analytic results.

Fig. 6. ϵ_y/y_c^2 due to linear coupling vs. N_{corr} in the ALS.

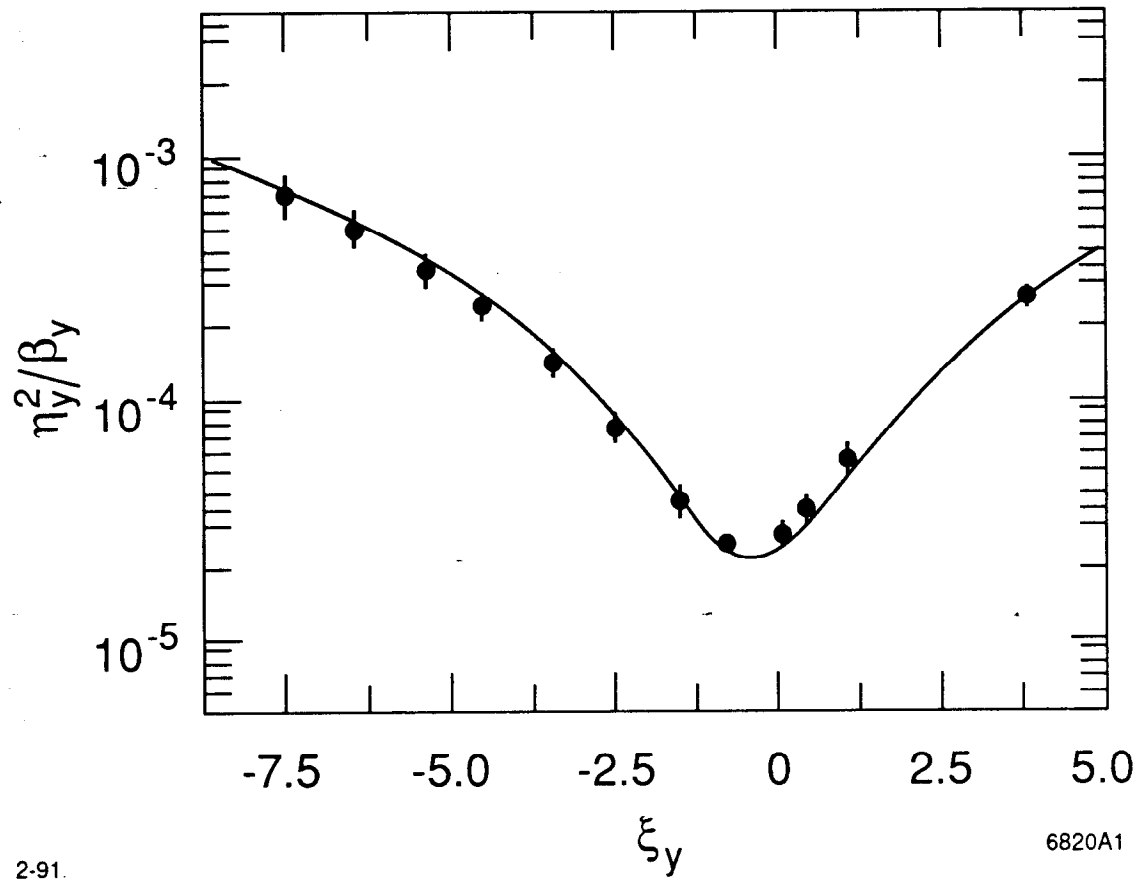
Fig. 7. Moments of the distribution for ϵ_y from dispersion due to random errors.

Fig. 8. Events vs. ϵ_y due to the vertical dispersion in the NDR1 lattice. Data is calculated from 1000 simulations of random vertical sextupole misalignments with ring tunes of: (a) $\nu_y = 3.07$, (b) $\nu_y = 3.275$, (c) $\nu_y = 3.43$, and (d) $\nu_y = 3.275$ after global correction.

Fig. 9. 95% confidence level for ϵ_y due to dispersion vs. the fractional tune.

Fig. 10. Events vs. ϵ_y due to the linear coupling in the NDR1 lattice. Data is calculated from 1000 simulations of random vertical sextupole misalignments for tunes of: (a) $\Delta\nu_+ = 0.35$ and $\Delta\nu_- = 0.10$, and (b) $\Delta\nu_+ = 0.35$ and $\Delta\nu_- = 0.50$.

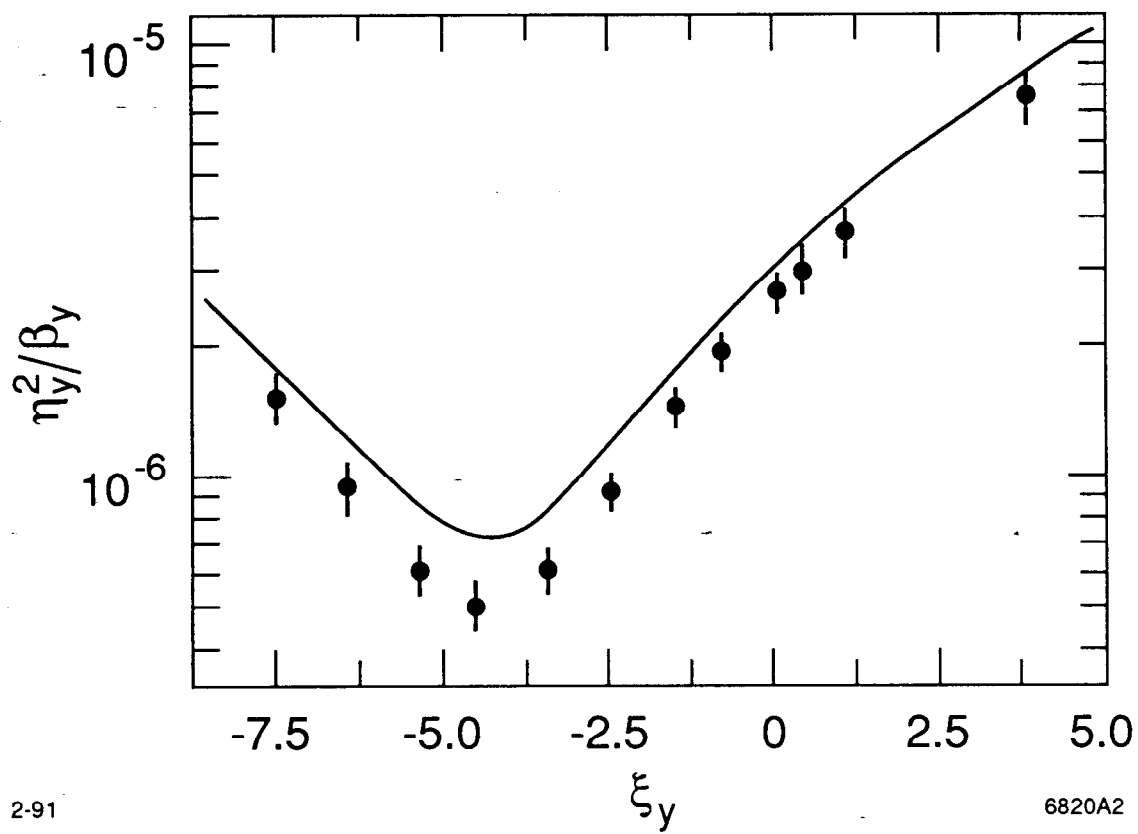
Fig. 11. 95% confidence level for ϵ_y due to betatron coupling vs. the distance from the difference coupling resonance for $\Delta\nu_+ = .35$.



2-91.

6820A1

Fig. 1



2-91

6820A2

Fig. 2

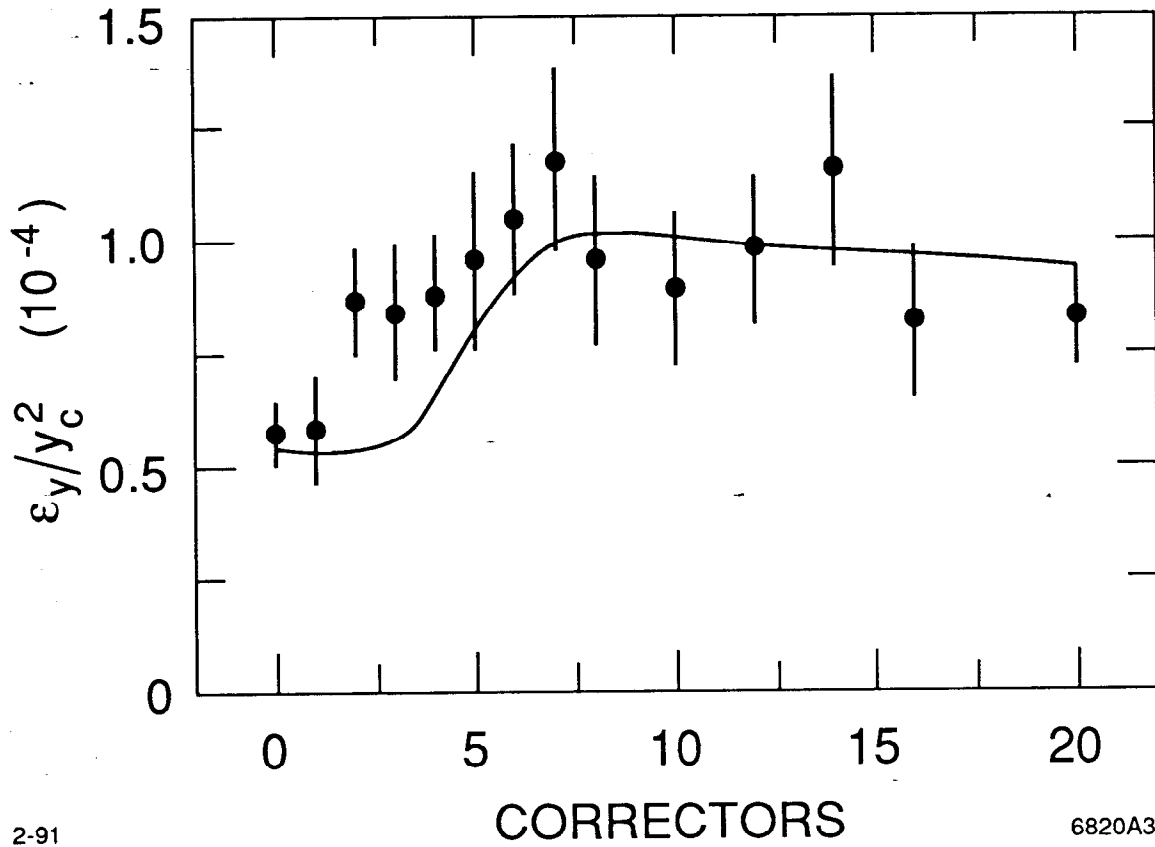
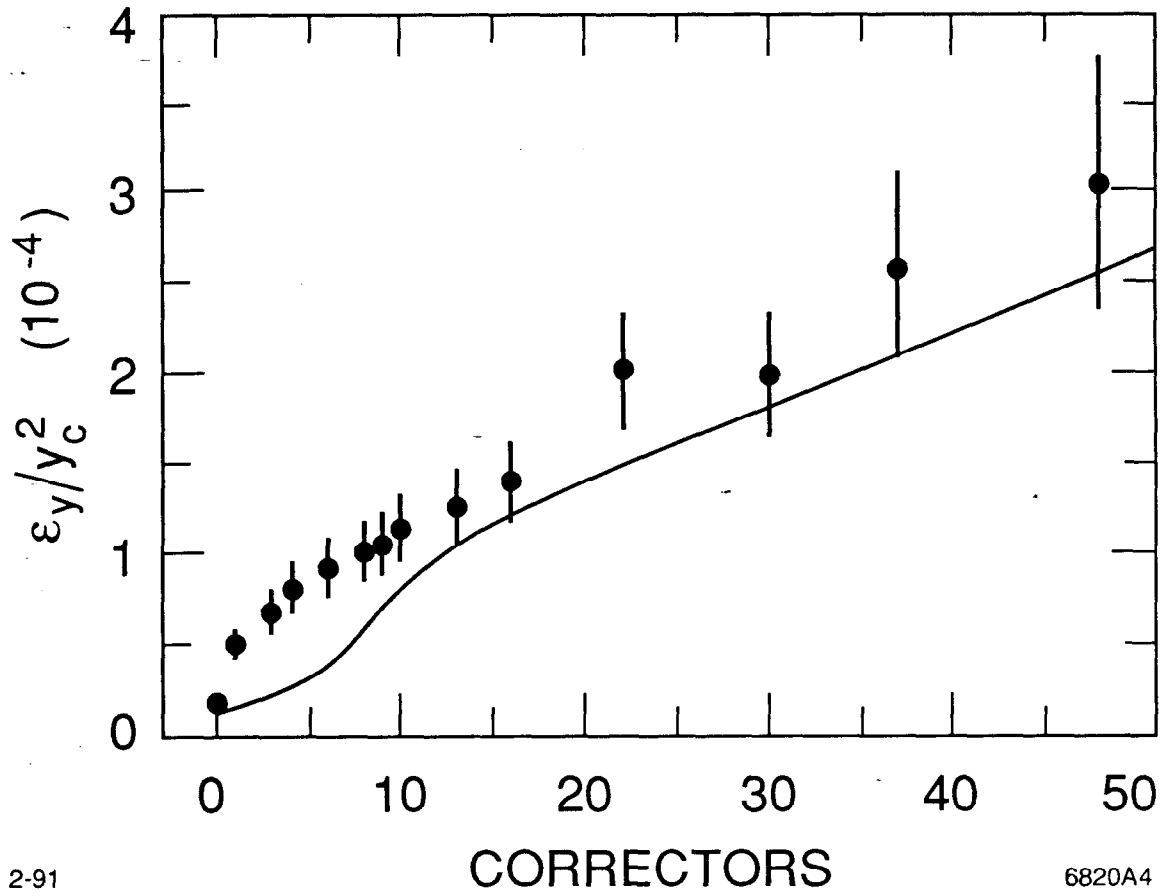


Fig. 3



2-91

6820A4

Fig. 4

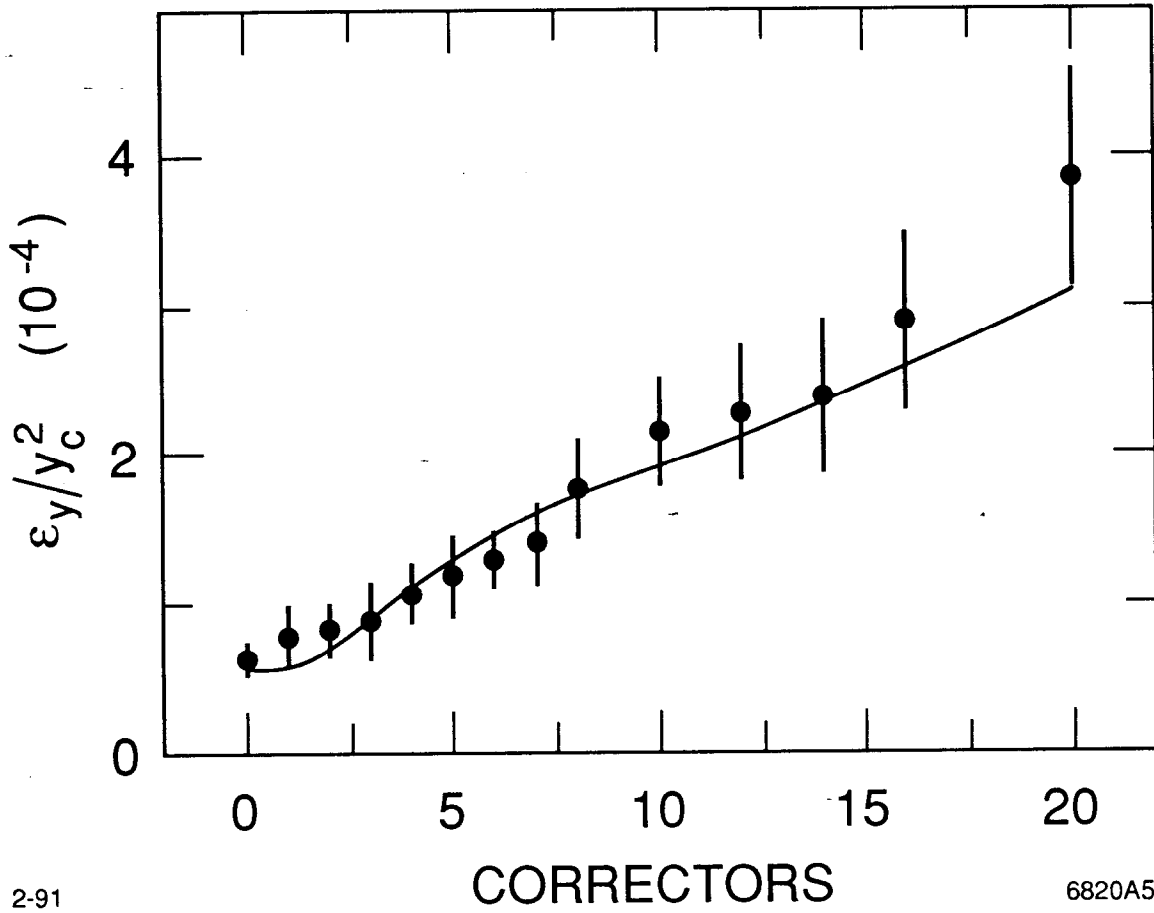
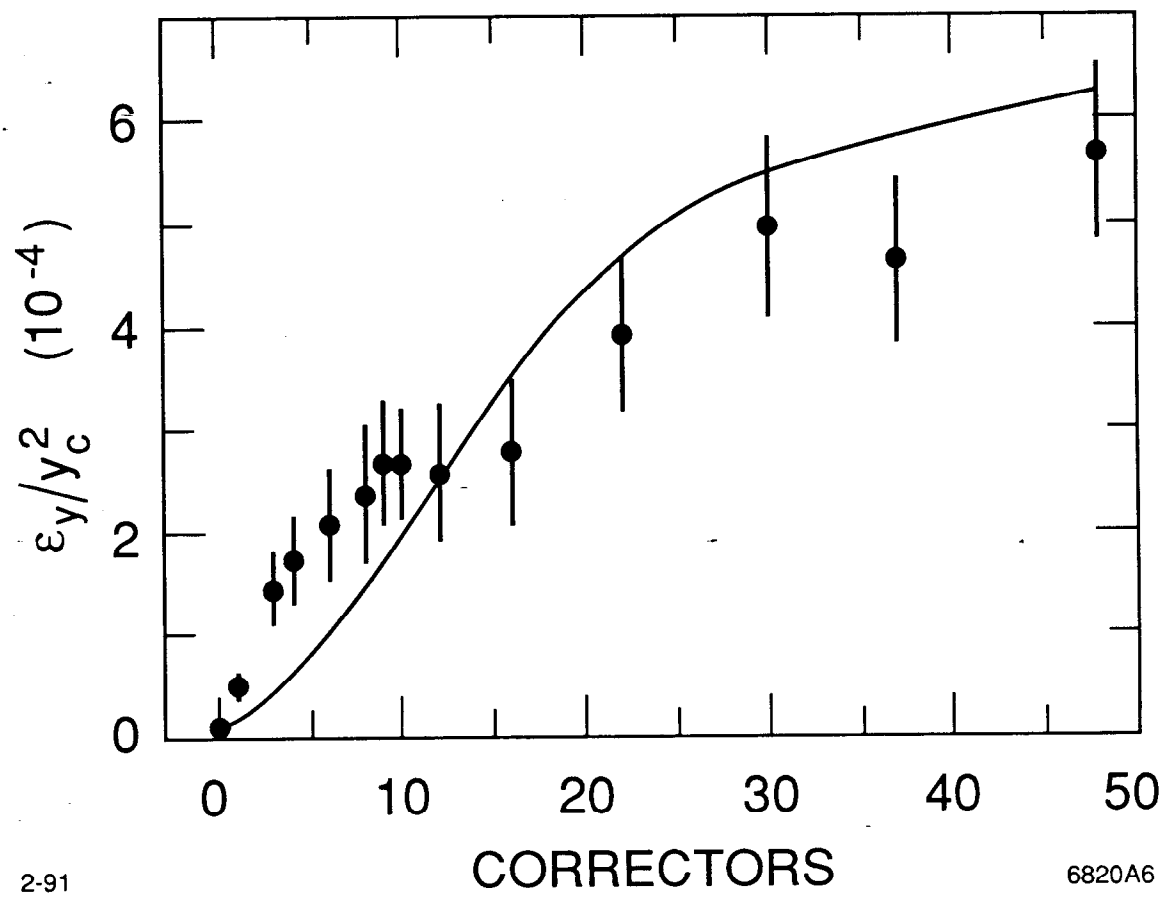


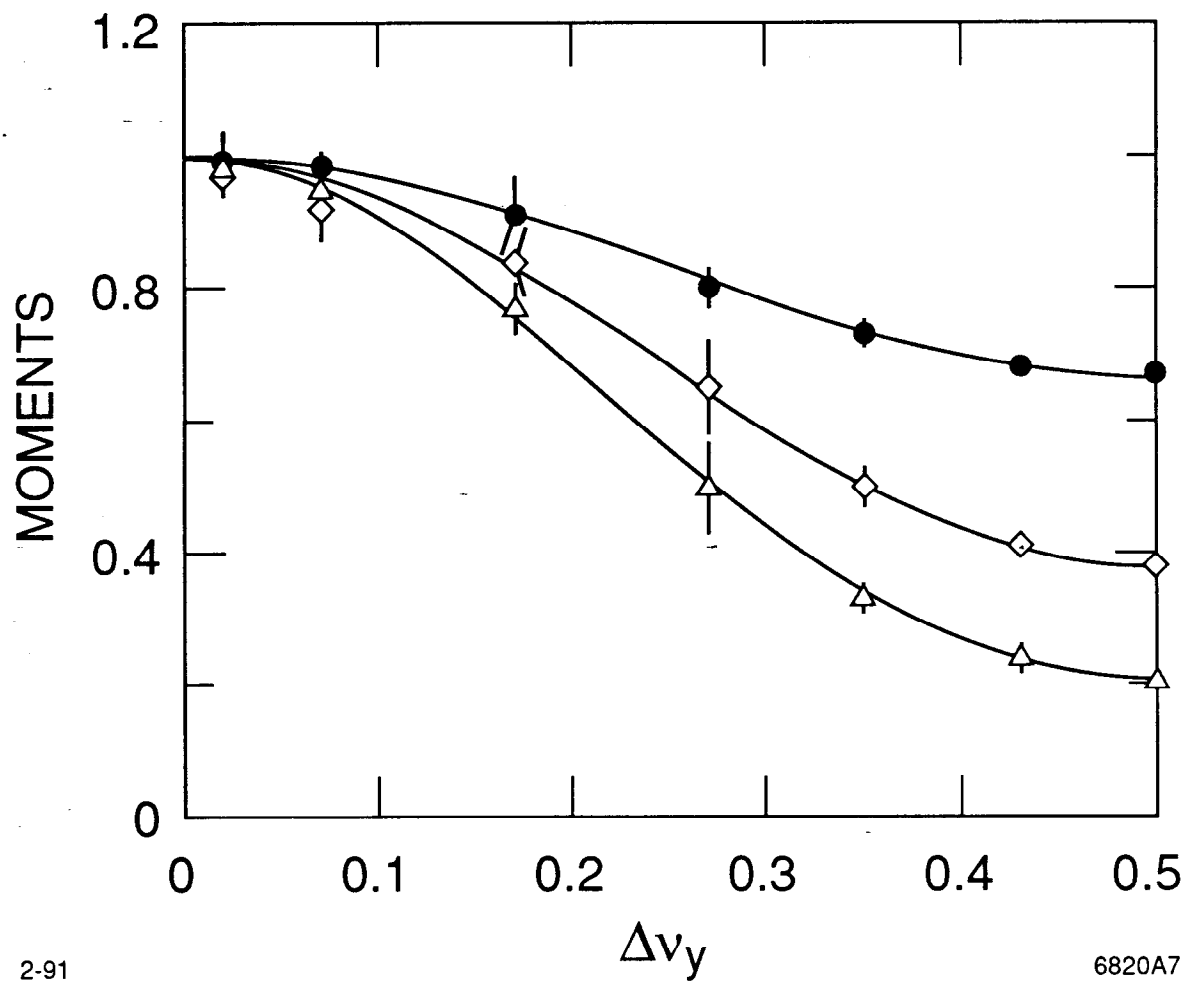
Fig. 5



2-91

6820A6

Fig. 6



2-91

6820A7

Fig. 7

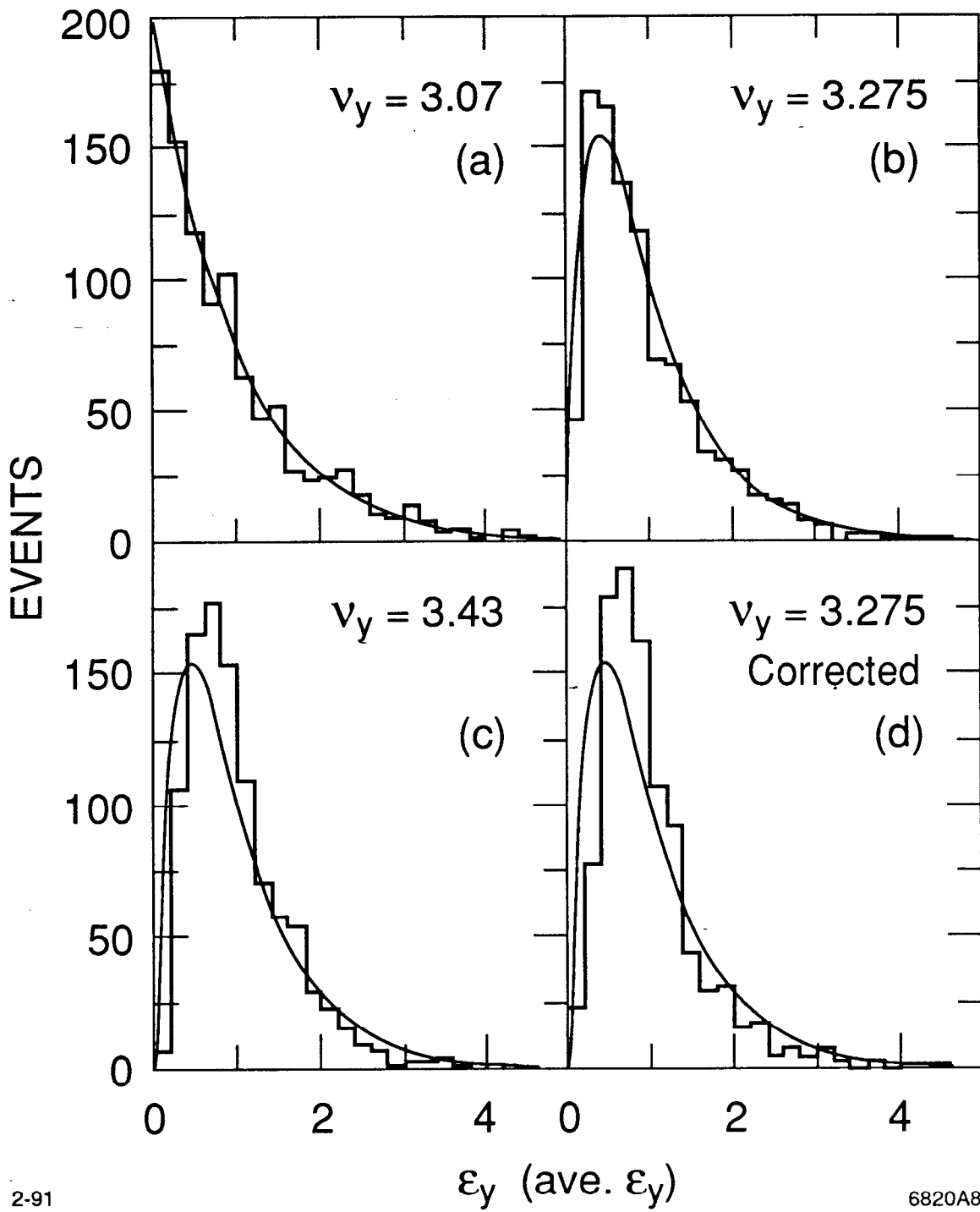
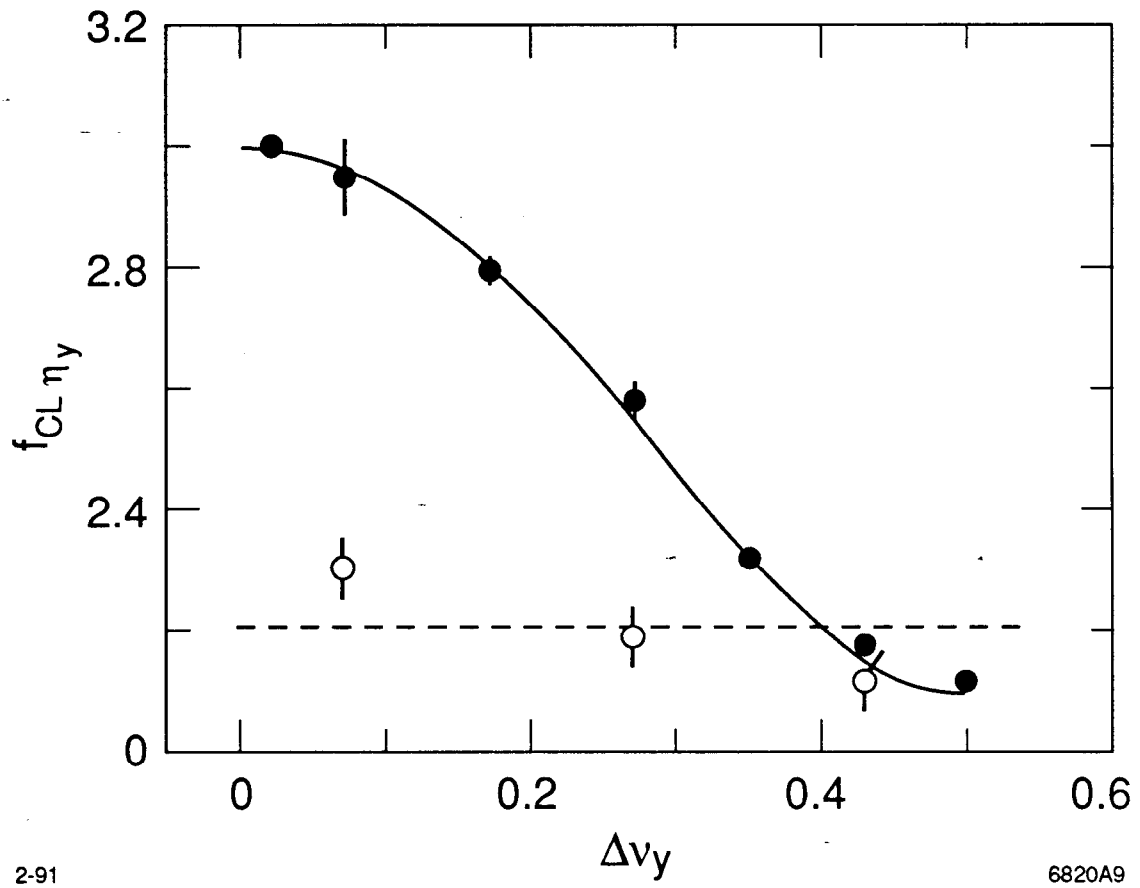


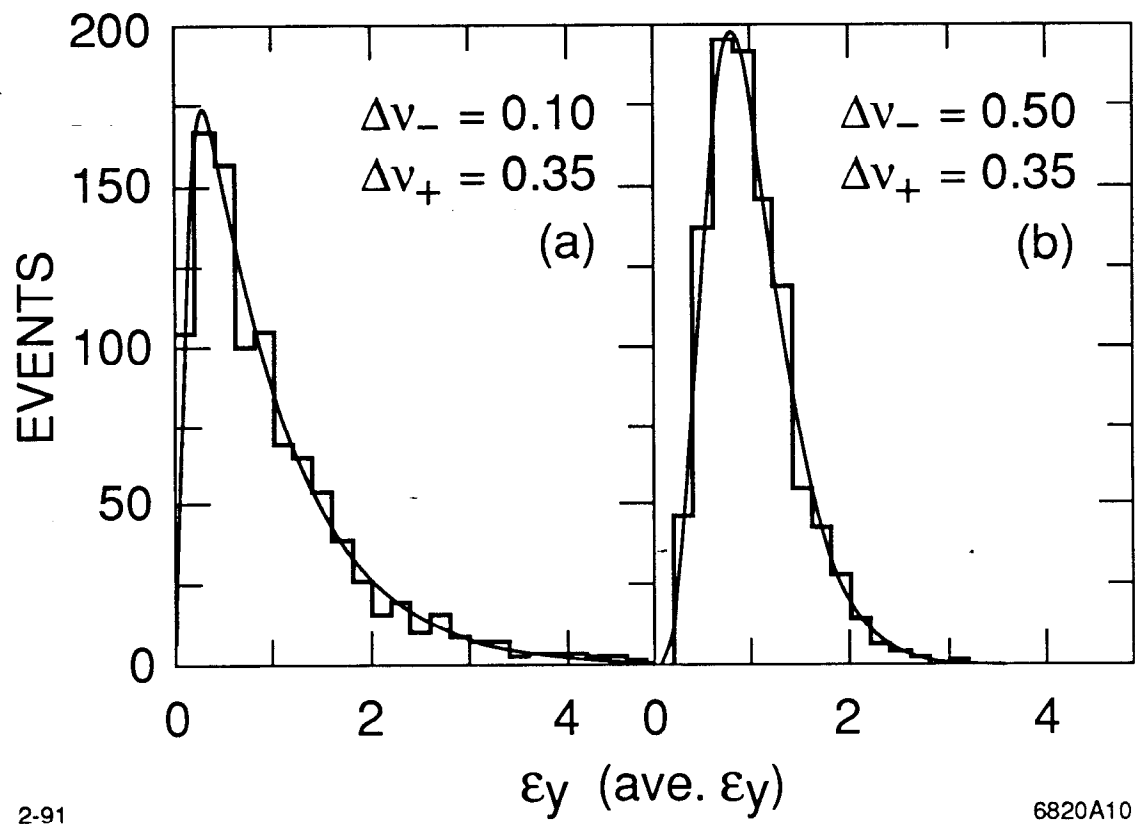
Fig. 8



2-91

6820A9

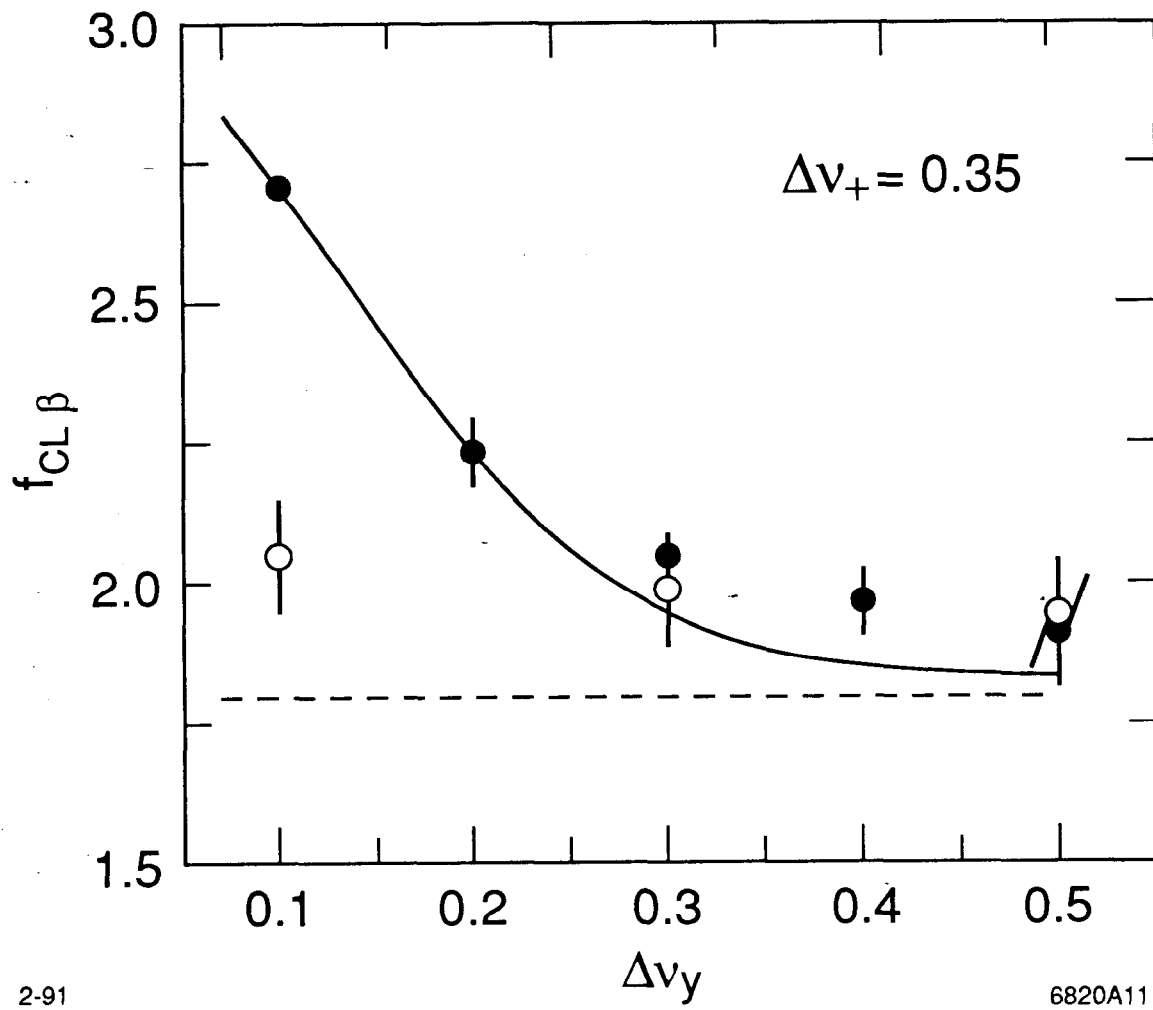
Fig. 9



2-91

6820A10

Fig. 10



2-91

6820A11

Fig. 11